國 立 交 通 大 學

電信工程研究所

碩 士 論 文

運用傳送功率分配於欠定多輸入多輸出系統達到公平傳輸速率

Achieving Fair Rate by Transmit Power Allocation for Underdetermined MIMO Systems

研 究 生：溫振鵬　　Student: Chen-Peng Wen

指導教授：李大嵩 博士　　Advisor: Dr. Ta-Sung Lee

中 華 民 國 九十九 年 六 月

運用傳送功率分配於欠定多輸入多輸出系統達到公平傳輸速率

Achieving Fair Rate by Transmit Power Allocation for Underdetermined MIMO Systems

研 究 生：溫振鵬　　Student: Chen-Peng Wen

指導教授：李大嵩 博士　　Advisor: Dr. Ta-Sung Lee

國立交通大學

電信工程研究所

碩士論文

A Thesis
Submitted to Institute of Communication Engineering
College of Electrical and Computer Engineering
National Chiao Tung University
in Partial Fulfillment of the Requirements
for the Degree of
Master
in
Communication Engineering
June 2010
Hsinchu, Taiwan, Republic of China

中 華 民 國 九 十 九 年 六 月

運用傳送功率分配於欠定多輸入多輸出系統達到公平傳輸速率

學生：溫振鵬　　指導教授：李大嵩 博士

國立交通大學電信工程研究所碩士班

摘要

在無線通訊系統中，多輸入多輸出技術不需額外頻寬及傳輸功率即能提高傳輸速率及改善傳輸品質。然而，在多用戶多輸入多輸出上鏈系統的環境中，由於部分用戶可能距離基地台較遠或被障礙物所阻擋，以致通道增益較小，導致傳輸速率變差。在本篇論文中，吾人提出一個傳送功率分配法達到公平的傳輸速率。吾人將一非線性最佳化問題轉換成適當形式，將之套用到現有的演算法中。此公平化的機制可使得等效子通道增益較為均勻，因此等效通道矩陣會傾向於良置（well-conditioned）。因為在欠定多輸入多輸出系統中，有效率的解碼器均基於球體解碼器，因此通道矩陣有較小的條件數（condition number），可使得解碼的複雜度降低。最後，吾人亦提出另一功用函數用於改善條件數，進一步降低運算複雜度。模擬結果顯示吾人提出方法的有效性。

Achieving Fair Rate by Transmit Power Allocation for Underdetermined MIMO Systems

Student: Chen-Peng Wen Advisor: Dr. Ta-Sung Lee

Institute of Communication Engineering

National Chiao Tung University

Abstract

In wireless communication systems, multiple-input multiple-output (MIMO) technology offers significant increases in data rate and link range without additional bandwidth and transmit power. However, in uplink multi-user MIMO systems, some users will suffer from small channel gains due to being far away from the base station or blocked by obstacles in practical environments. This result in poor data rates for those users. In this thesis, we propose a transmit power allocation scheme with fair rate allocation for all users. We reformulate a nonlinear optimization problem to a modified form which can be applied to the existing algorithms. The proposed fairness scheme also leads to uniform sub-channel gains. Thus the equivalent channel matrix will tend to be well-conditioned. Since efficient decoders of underdetermined MIMO systems are based on sphere decoders, the decoding complexity can be reduced with a smaller channel condition number. Finally, we also propose an alternative utility function to improve the condition number, to further reduce the decoding complexity. Simulation results confirm the effectiveness of the proposed methods.

Acknowledgement

I would like to express my deepest gratitude to my advisors, Dr. Ta-Sung Lee for his enthusiastic guidance and great patience, especially in the training of presentation. I learned a lot from his positive attitude in many areas. Thanks are also offered to all members in the Communication System Design and Signal Processing (CSDSP) Lab. Last but not least, I would like to show my sincere thanks to my family for their invaluable love and support.

Table of Contents

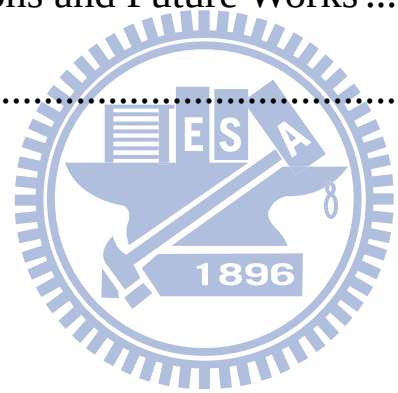

List of Figures

Acronym Glossary

D-BLAST	diagonal Bell laboratories layered space-time
EGC	equal-gain combining
GSD	Generalized Sphere Decoding
MIMO	multiple-input multiple-output
MISO	multiple-input-single-output
ML	maximum-likelihood
MRC	maximum ratio combining
MU-MIMO	multi-user multiple-input multiple-output
SDA	sphere decoding algorithm
SIC	successive interference cancellation
SIMO	single-input-multiple-output
SISO	single-input-single-output
SNR	signal to noise ratio
SINR	signal to interference plus noise ratio
SSD	slab sphere decoding
STBC	space-time block code
STC	space-time code
STTC	space-time trellis code
SU-MIMO	single-user multiple-input multiple-output
V-BLAST	vertical Bell laboratories layered space-time

Notations

$(\cdot)^{-1}$	inverse operator
$(\cdot)^{T}$	transpose operator
$E\{\cdot\}$	expectation operator
$(\cdot)^{\dagger}$	Moore-Penrose pseudo-inverse operator
C	channel capacity
$\mathbf{H}$	channel matrix
M_r	number of receive antennas
N_t	number of transmit antennas
$\mathbf{n}$	noise vector
γ	average SNR at the receiver
$\mathbf{x}$	transmit signal vector
$\mathbf{y}$	received signal vector

Chapter 1

Introduction

Next generation wireless communication systems are expected to provide users with higher data rate services including video, audio, data and voice signals. The rapidly growing demand for these services drives the wireless communication technologies towards higher data rate, higher mobility and higher link quality. However, the time-selective and frequency-selective fading in wireless channel caused by multipath propagation, Doppler shifts and carrier frequency/phase drifts severely affect the quality and reliability of wireless communication. Besides, the available bandwidth and power are limited which makes the design of wireless communication systems extremely challenging. Hence, recently there are many innovative techniques that improve the reliability and the spectral efficiency of wireless communication links. Some popular examples include the coded multicarrirer modulation, smart antenna, in particular multiple-input multiple-output (MIMO) technology [1-4] and adaptive modulation [5], [6].

MIMO technology involves the use of multiple antennas at the transmitter and receiver to improve communication performance. The technology offers some benefits that overcome the challenges posed by both the impairments in wireless channel as well as resource constraints. The two important benefits of MIMO

technology are the diversity gain and the spatial multiplexing gain. Diversity gain mitigates fading by providing the receiver with multiple (ideally independent) copies of the transmitted signal in space, time or frequency. Spatial multiplexing offers a linear increase in data rate by transmitting multiple independent data streams within the bandwidth of operation.

There are many signal detection schemes for MIMO systems such as linear detection, successive interference cancellation (SIC) [7], [8] and the maximum-likelihood (ML) detection. Both linear detection and the SIC schemes are easy to be implemented but their detection performances are not optimal. The optimal detection scheme is ML detection; however, the complexity of the ML detection scheme grows exponentially with the size of the transmit symbol alphabet and the number of transmit antennas. To reduce the complexity of ML detection, the sphere decoding algorithm (SDA) is introduced in [9-12] to achieve the same performance as ML detection with reduced complexity. The basic idea of SDA is to search the nearest lattice point to the received signal vector within a given sphere radius. However, the typical SDA fails to decode in underdetermined MIMO systems. Thus several algorithms are proposed to decode the underdetermined MIMO systems, including Generalized Sphere Decoding (GSD) algorithm [13], Slab Sphere Decoding (SSD) algorithm [14-16], and Regularization Method [17].

In uplink multi-user MIMO (MU-MIMO) systems, if the number of users is larger than the number of base station antennas, then it can be regarded as an underdetermined MIMO system. Considering in the practical environments, some users will suffer from small channel gains due to being far away from the base station or blocked by obstacles. This results in poor data rates for those users. The waterfilling power allocation algorithm in [18] can provide a maximum throughput of the systems, but the data rate for the user with small channel gain will be severely

degraded..

In this thesis, our major goal is to achieve fair data rates for all users. We propose a transmit power allocation to realize this. And we reformulate a nonlinear optimization problem into a modified form which can be applied to the existing algorithms. The proposed fairness scheme also leads to uniform sub-channel gains. Thus the equivalent channel matrix will tend to be well-conditioned. We further propose a determinant based utility function to improve the condition number. Thus the complexity of the SDA based decoder can be reduced.

The remainder of the thesis is organized as follows. In Chapter 2, The signal model of the MIMO systems is introduced first. Secondly, several algorithms for decoding underdetermined MIMO systems are presented. In Chapter 3, the proposed transmit power allocation scheme is developed. Discussion on the condition number and the determinant based utility function will be described in Chapter 4. Simulation results of the proposed methods are also illustrated in this chapter. Finally, we summarize the contributions of our works and give some potential future works in Chapter 5.

Chapter 2

MIMO Systems

In wireless communications, one can improve communication performance by using multiple-input and multiple-output (MIMO) technology. MIMO offers significant increases in data rate and link reliability without additional bandwidth or transmit power. In this chapter, we give a review of MIMO systems. We first introduce the MIMO system model in Section 2.1. Section 2.2 introduces the channel capacity. Then, the spatial diversity and the spatial multiplexing techniques are introduced in Section 2.3 and Section 2.4, respectively. The generalized sphere decoding (GSD) algorithms have been studied as a solution to the ML detection for underdetermined MIMO systems with reduced complexity. We will give an introduction of the GSD algorithms in Section 2.5.

2.1 System Model

Figure 2-1 shows the typical multiple-input-multiple-output (MIMO) system with N_t transmit antennas and M_r receive antennas. The frequency-flat fading channel matrix $\widetilde{\mathbf{H}}$ can be written as

$$\widetilde{\mathbf{H}} = \begin{bmatrix} \tilde{h}_{11} & \tilde{h}_{12} & \cdots & \tilde{h}_{1N_t} \\ \tilde{h}_{21} & \tilde{h}_{22} & \cdots & \tilde{h}_{2N_t} \\ \vdots & \vdots & \ddots & \vdots \\ \tilde{h}_{M_r1} & \tilde{h}_{M_r2} & \cdots & \tilde{h}_{M_rN_t} \end{bmatrix} \in \mathbb{C}^{M_r \times N_t}, \tag{2.1}$$

where the elements of $\widetilde{\mathbf{H}}$ are i.i.d. complex Gaussian random variables with zero-mean and unit variance. The relation between the transmitted signal vector and received signal vector can be written as

$$\tilde{\mathbf{y}} = \widetilde{\mathbf{H}}\tilde{\mathbf{x}} + \tilde{\mathbf{n}}, \tag{2.2}$$

where $\tilde{\mathbf{y}} = \left[\tilde{y}_1, \tilde{y}_2, \cdots, \tilde{y}_{M_r}\right] \in \mathbb{C}^{M_r \times 1}$ and $\tilde{\mathbf{x}} = \left[\tilde{x}_1, \tilde{x}_2, \cdots, \tilde{x}_{N_t}\right] \in \mathbb{C}^{N_t \times 1}$ are the received signal vector and transmitted signal vector , respectively. $\tilde{\mathbf{n}} = \left[\tilde{n}_1, \tilde{n}_2, \cdots, \tilde{n}_{M_r}\right] \in \mathbb{C}^{M_r \times 1}$ denotes the i.i.d. complex additive white Gaussian noise (AWGN) vector with zero-mean and covariance matrix $\sigma^2\mathbf{I}$. When $M_r > N_t$, the system is called an overdetermined MIMO system. When $M_r < N_t$, it is called an underdetermined MIMO system.

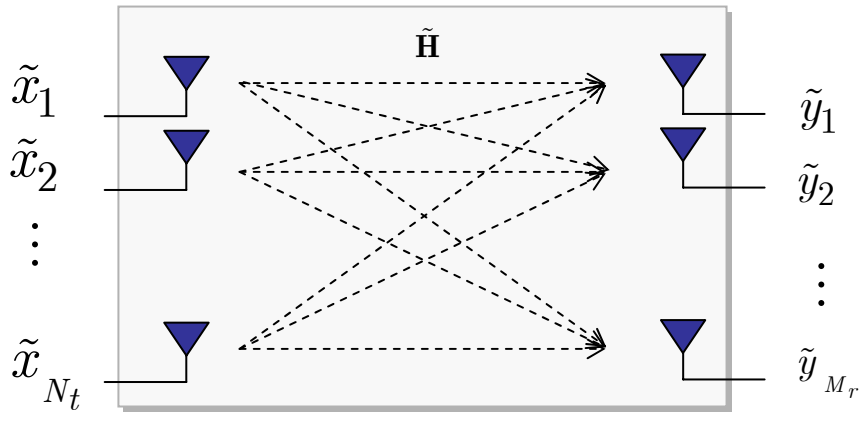

Fig. 2-1 MIMO system

The complex MIMO system can be transformed into an equivalent real system. By using the real-value decomposition, (2.2) can be written as

$$\mathbf{y} = \mathbf{H}\mathbf{x} + \mathbf{n}\,, \tag{2.3}$$

where

$$\mathbf{y} = [\mathrm{Re}\{\tilde{\mathbf{y}}\}^T\ \mathrm{Im}\{\tilde{\mathbf{y}}\}^T] \in \mathbb{R}^M,$$
$$\mathbf{x} = [\mathrm{Re}\{\tilde{\mathbf{x}}\}^T\ \mathrm{Im}\{\tilde{\mathbf{x}}\}^T] \in \mathbb{R}^N,$$
$$\mathbf{n} = [\mathrm{Re}\{\tilde{\mathbf{n}}\}^T\ \mathrm{Im}\{\tilde{\mathbf{n}}\}^T] \in \mathbb{R}^M,$$

and

$$\mathbf{H} = \begin{bmatrix} \mathrm{Re}\left\{\widetilde{\mathbf{H}}\right\}^T & -\mathrm{Im}\left\{\widetilde{\mathbf{H}}\right\}^T \\ \mathrm{Im}\left\{\widetilde{\mathbf{H}}\right\}^T & \mathrm{Re}\left\{\widetilde{\mathbf{H}}\right\}^T \end{bmatrix} \in \mathbb{R}^{M\times N}.$$

Note that the dimension of $\mathbf{H}$ is $M \times N$ where $M = 2 \times M_r$ and $N = 2 \times N_t$.

2.2 Channel Capacity

Channel capacity is the highest rate in bits per channel use at which information can be transmitted with an arbitrary probability of error. We first introduce the single-input-single-output (SISO) channel capacity and then study the capacity of a MIMO channel. Note that single-input-multiple-output (SIMO) and multiple-input-single-output (MISO) channel are sub-sets of the MIMO case. The channel capacity is defined as [19]

$$C = \max_{p(x)} \mathrm{I}(X;Y), \tag{2.4}$$

where

$$\mathrm{I}(X;Y) = \mathrm{H}(Y) - \mathrm{H}(Y \mid X), \tag{2.5}$$

is the mutual information between X and Y, $\mathrm{H}(Y)$ and $\mathrm{H}(Y \mid X)$ are the differential entropy of Y and differential conditional entropy of Y with knowledge of X given, respectively. In (2.4), it states that the mutual information is maximized with respect

to all possible transmitter statistical distributions $p(x)$.

The ergodic capacity of a SISO system with a random complex channel gain h is given by [19]

$$C = E\left\{\log_2(1+\gamma|h|^2)\right\} \quad \text{bits/sec/Hz,} \tag{2.6}$$

where $\gamma = P/\sigma^2$ is the average SNR at the receiver, P is the transmit power and E{x} is denotes the expectation over all channel realizations. For a MIMO system with N transmit antennas and M receive antennas, the capacity of a random MIMO channel is given by [1]

$$C = \max_{tr(\mathbf{R}_{xx})=N} E\left\{\log_2\left[\det(\mathbf{I}_M + \frac{P}{\sigma^2 N}\mathbf{H}\mathbf{R}_{xx}\mathbf{H}^H)\right]\right\} \quad \text{bits/sec/Hz,} \tag{2.7}$$

where $\mathbf{R}_{xx} = E\left\{\mathbf{x}\mathbf{x}^H\right\}$ is the covariance matrix of the transmitted signal vector $\mathbf{x}$. If the channel knowledge is unknown to the transmitter, the signals are chosen to be independent and equal power. The covariance matrix of the transmit signal vector is then given by $\mathbf{R}_{xx} = \mathbf{I}_M$. As a result, the ergodic capacity of a MIMO system can be written as [1]

$$C = E\left\{\log_2\left[\det(\mathbf{I}_M + \frac{P}{\sigma^2 N}\mathbf{H}\mathbf{R}_{xx}\mathbf{H}^H)\right]\right\} \quad \text{bits/sec/Hz,} \tag{2.8}$$

By using the eigenvalue decomposition, the matrix product of $\mathbf{H}\mathbf{H}^H$ can be decomposed as $\mathbf{H}\mathbf{H}^H = \mathbf{E}\Lambda\mathbf{E}^H$, where $\mathbf{E}$ is an $M \times M$ matrix which consists of the eigenvectors satisfying $\mathbf{E}\mathbf{E}^H = \mathbf{E}^H\mathbf{E} = \mathbf{I}_M$ and $\Lambda = \text{diag}\{\lambda_1, \lambda_2, \ldots, \lambda_M\}$ is a diagonal matrix with the eigenvalues $\lambda_i \geq 0$ on the main diagonal. Assuming that the eigenvalues λ_i are ordered so that $\lambda_i \geq \lambda_{i+1}$, we have

$$\lambda_i = \begin{cases} \sigma_i^2, & \text{if } 1 \leq i \leq r \\ 0, & \text{if } r+1 \leq i \leq M \end{cases}, \tag{2.9}$$

where σ_i^2 is the ith squared singular value of the channel matrix $\mathbf{H}$ and $r = \mathrm{rank}(\mathbf{H}) \le \min\{N, M\}$ is the rank of the channel matrix. Then the capacity of a MIMO channel can hence be rewritten as

$$\begin{aligned} C &= E\left\{\log_2\left[\det(\mathbf{I}_M + \frac{P}{\sigma^2 N}\mathbf{E}\Lambda\mathbf{E}^H)\right]\right\} = E\left\{\log_2\left[\det(\mathbf{I}_M + \frac{P}{\sigma^2 N}\Lambda)\right]\right\} \\ &= \sum_{i=1}^{r} E\left\{\log_2\left[\det(1 + \frac{P}{\sigma^2 N}\lambda_i)\right]\right\} \quad \text{bits/sec/Hz} \end{aligned}, \quad (2.10)$$

Note that the second equation holds due to the fact $\det(\mathbf{I}_m + \mathbf{AB}) = \det(\mathbf{I}_n + \mathbf{BA})$ for matrices $\mathbf{A} \in \mathbb{C}^{m\times n}$ and $\mathbf{B} \in \mathbb{C}^{m\times n}$ and $\mathbf{E}^H\mathbf{E} = \mathbf{I}_M$. (2.10) shows that the capacity of a MIMO channel is made up by sum of the capacities of r SISO sub-channels with power gain λ_i for i=1,2,…,r and transmit power P/N individually.

If the channel knowledge is known to the transmitter, the capacity of a MIMO channel is the sum of the capacities associated with the parallel SISO channels and is given by

$$C = \sum_{i=1}^{r} E\left\{\log_2\left[\det(1 + \gamma_i \frac{P}{\sigma^2 N}\lambda_i)\right]\right\} \quad \text{bits/sec/Hz}, \quad (2.11)$$

where $\gamma_i = E\left\{|x_i|^2\right\}$ for i=1,2,…,r is the transmit power in the ith sub-channel and satisfy $\sum_{i=1}^{r}\lambda_i = N$. Since the transmitter can access the spatial sub-channels, we can allocate variable power across the sub-channels to maximize the mutual information. The optimal power allocation of the ith sub-channel is given by [1], [19]

$$\gamma_i^{\mathrm{opt}} = \left(\mu - \frac{M\sigma^2}{P\lambda_i}\right)_+ \quad \text{for } i = 1,2,\cdots,r, \quad (2.12)$$

where μ is chosen to satisfy the constraint $\sum_{i=1}^{r}\gamma_i^{\mathrm{opt}} = N$ and $(\cdot)_+$ denotes the operation that taking those terms which are positive. The optimal power allocation in

(2.12) is found iteratively through the water-filling algorithm [1], [19].

2.3 MIMO Diversity

Diversity techniques are widely used in MIMO systems to improve the reliability of transmission without increasing the transmit power or sacrificing the bandwidth. There are many diversity techniques such as time diversity, frequency diversity and space diversity. In this section we focus on the space diversity that is so called antenna diversity.

2.3.1 Receive Diversity

Receive diversity involves the use of multiple antennas at the receiver. At the receiver, multiple copies of the transmitted signal are received, which can be efficiently combined with an appropriate signal processing algorithm. There are four main types of combining techniques, include selection combing, switch combining, equal-gain combining (EGC) and the maximum ratio combining (MRC). In the selection combining, the received signal with the best quality is chosen and the choosing criterion is based on SNR. Switch diversity switches the received signal path to an alternative antenna when the current received signal level falls below a given threshold. EGC is a simple method since it does not require estimation of the channel. The receiver simply combines the received signals from different receive antennas with weights set to be equal. MRC forms the output signal by a linear combination of all the received signals and is the optimal combination technique which achieves the maximum value of the output SNR.

2.3.2 Transmit Diversity

Transmit diversity techniques which provide diversity benefits at the receiver with multiple transmit antennas, has received much attention, especially in wireless cellular systems. There are two broad categories of transmit diversity: the open loop schemes and the closed loop schemes. In the open loop schemes, the transmitter transmits signals without feedback information from receiver. Space-time code (STC) is an open loop scheme which jointly designs of channel coding and modulation to improve system performance by providing both transmit diversity and coding gain. STC can be classified into two categories, the space-time block code (STBC) and the space-time trellis code (STTC).

2.4 Spatial Multiplexing

Spatial multiplexing is a transmission technique of MIMO wireless communication systems which increases the transmission data rate without additional bandwidth or power consumption. In the spatial multiplexing systems, N different data streams are transmitted from different transmit antennas simultaneously or sequentially and these data streams are separated and demutiplexed to yield the original transmitted signals according to their unique spatial signatures at the receiver, as illustrated in Fig. 2-2. The separation of data streams at the receiver can be done possibly by the fact that rich scattering multi-paths contribute to lower correlations between MIMO channel coefficients and hence create a channel matrix with full rank and low condition number to N unknowns from a linear system of M equations. In the following, two typical spatial multiplexing schemes, D-BLAST [4] and V-BLAST [20] are introduced.

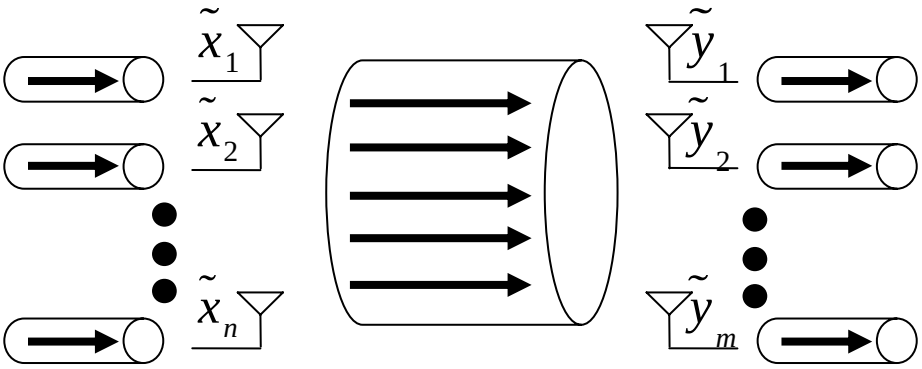

Fig. 2-2 Spatial multiplexing system

(1) Diagonal Bell Laboratories Layered Space-Time (D-BLAST)

The concept of layered space-time processing was introduced by Foschini at Bell Laboratories [4]. D-BLAST uses multiple antennas at both the transmitter and the receiver, and an elegant diagonally-layered coding sequence in which code blocks are dispersed across the diagonals in space-time. The high-rate information bit stream is first demultiplexed into *N* substreams, and each substream is encoded by a conventional 1-D constituent code. The encoders apply these coded symbols to the input to form a semi-infinite matrix **X** of *N* rows to be transmitted. The encoding procedure is shown in Fig. 2-3.

(2) Vertical Bell Laboratories Layered Space-Time (V-BLAST)

The D-BLAST algorithm suffers from certain implementation complexities which is not suitable for practical implementation. Therefore, a simplified version of the BLAST algorithm is known as V-BLAST. It is capable of achieving high spectral efficiency while being relatively simple to be implemented. The coding procedure of the V-BLAST can be viewed as there is an encoder on each transmit antenna. The output coded symbols of each encoder are transmitted directly from the corresponding antenna which is shown in Fig. 2-4.

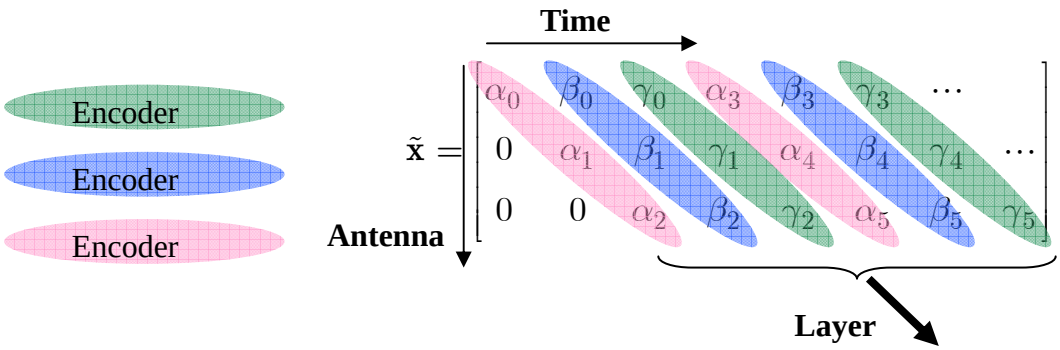

Fig. 2-3 Encoding procedure of D-BLAST (n=3)

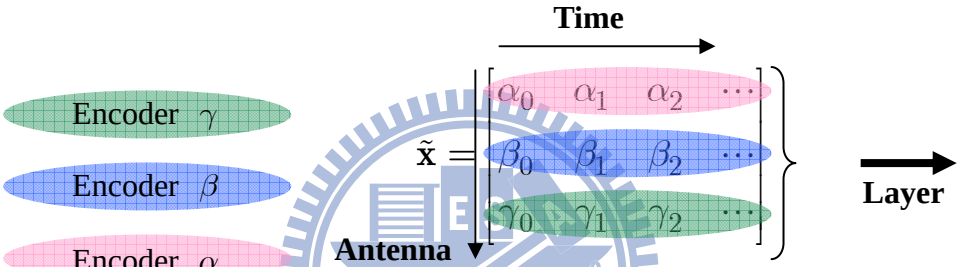

Fig. 2-4 Encoding procedure of V-BLAST (n=3)

2.5 Underdetermined MIMO Decoder

Maximum-likelihood (ML) detection complexity increases exponentially depending on the number of transmit antennas and the constellation size. Hence, it is a serious issue in designing the receiver in recent years. In order to reduce the complexity of ML detection, the sphere decoding algorithms (SDA) [9-12] are proposed to solve the problem and achieve the ML performance. But the SDA fails in the underdetermined MIMO systems. There are several algorithms that can solve the underdetermined problem, such as Generalized Sphere Decoding (GSD) [13] algorithm, Slab Sphere Decoding (SSD) [14-16] algorithm, and Regularization

Method [17]. We introduce these algorithms in this section.

2.5.1 GSD algorithm

Consider a MIMO system with N_t transmit antennas and M_r receive antennas. The received real signal can be written as (2.3):

$$\mathbf{y} = \mathbf{H}\mathbf{x} + \mathbf{n}.$$

The ML estimator $\hat{\mathbf{x}}$ of $\mathbf{x}$ is obtained by minimizing the Euclidean distance of $\mathbf{y}$ from the legal lattice points can be represented as

$$\hat{\mathbf{x}} = \arg\min_{\mathbf{x}\in\mathbb{Z}^N} \|\mathbf{y} - \mathbf{H}\mathbf{x}\|^2 = \arg\min_{\mathbf{x}\in\mathbb{Z}^N} \|\mathbf{R}(\rho - \mathbf{x})\|^2. \tag{2.13}$$

where $\mathbb{Z} = \{\pm 1, \pm 3, \cdots, \pm(2^k\text{-}1)\}$ is the 4-QAM, 16-QAM, 64-QAM constellations for $k = 1,2,3$, respectively. $\rho = \mathbf{H}^T\left(\mathbf{H}\mathbf{H}^T\right)^{-1}\mathbf{y}$, $\mathbf{Q}$ is an $M \times M$ orthogonal matrix, and $\mathbf{R}$ is an $M \times N$ upper triangular matrix corresponding to the QR-decomposition of $\mathbf{H}$, i.e. $\mathbf{H} = \mathbf{Q}\mathbf{R}$. The matrix R can be represented as $\mathbf{R} = [\mathbf{R}_1, \mathbf{R}_2]$, where $\mathbf{R}_1 \in \mathbb{R}^{M\times M}$ is an upper triangular and $\mathbf{R}_2 \in \mathbb{R}^{M\times N-M}$. Similarly, $\mathbf{x}$ can be represented as $\mathbf{x} = \left[\mathbf{x}_G, \mathbf{x}_{\overline{G}}\right]^T$, where G and $\overline{G}$ are the indices corresponding to the first M and the last M -N elements of the $\mathbf{x}$. The minimum distance corresponding to the ML estimator in (2.13) can be rewritten as

$$\begin{aligned} &\arg\min_{\mathbf{x}\in\mathbb{Z}^N} \|\mathbf{R}(\rho - \mathbf{x})\|^2 \\ &= \min_{\mathbf{x}_{\overline{G}}\in\mathbb{Z}^{N-M}} \left(\min_{\mathbf{x}_G\in\mathbb{Z}^M} \left\| [\mathbf{R}_1, \mathbf{R}_2]\rho - \mathbf{R}_2\mathbf{x}_{\overline{G}} - \mathbf{R}_1\mathbf{x}_G \right\|^2 \right) \\ &= \min_{\mathbf{x}_{\overline{G}}\in\mathbb{Z}^{N-M}} \left(\min_{\mathbf{x}_G\in\mathbb{Z}^M} \left\| \tilde{\rho} - \mathbf{R}_1\mathbf{x}_G \right\|^2 \right), \end{aligned} \tag{2.14}$$

where $\tilde{\rho} = [\mathbf{R}_1, \mathbf{R}_2]\rho - \mathbf{R}_2\mathbf{x}_{\overline{G}}$.

The GSD checks all legal constellation points in a sphere with radius C. That means we set the squared Euclidean distance in (2.14) to be smaller than a positive number C^2. The problem can be solved by exhaustive search over $\mathbf{x}_{\overline{G}}$ and employing the SDA to compute the last equation in (2.14). The SDA algorithm finds the valid candidates if the squared minimum distance is less than C^2. Otherwise, a failure of the SDA for the given $\mathbf{x}_{\overline{G}}$ is declared and then the $\mathbf{x}_{\overline{G}}$ will be discarded.

If a candidate constellation point $(\mathbf{x}_G, \mathbf{x}_{\overline{G}})$ is found within the sphere, the value of C^2 is updated and the algorithm continues to search the remaining points for $\mathbf{x}_{\overline{G}}$. If no candidate constellation point is found within the sphere, then the entire algorithm is repeated with a value larger than the original radius C. The GSD is based on the exhaustive search over $\mathbf{x}_{\overline{G}}$ and each searched point should follow the SDA. Because of the exhaustive search over $\mathbf{x}_{\overline{G}}$, its complexity will exponentially increase depending on the size of $N-M$.

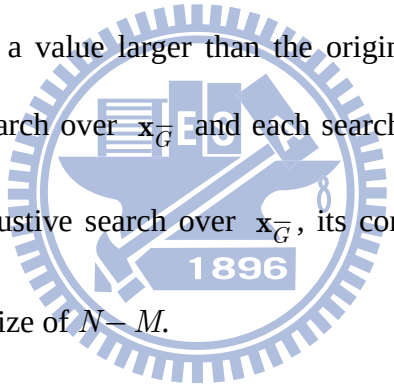

2.5.2 Slab Sphere Decoding (SSD) Algorithm

To perform (2.13) efficiently, an algorithm is proposed in [9], [20] to solve a search problem that finds all the lattice points satisfying

$$\|\mathbf{y} - \mathbf{H}\mathbf{x}\|^2 \leq C^2 \tag{2.15}$$

for given a radius $C\ (>0)$. Apparently, the point that is the closest to center of the hypersphere $\mathbf{y}$, is the ML decision point. By decomposing the channel using QR-decomposition, (2.15) can be rewritten as

$$\left\|\mathbf{y}' - \mathbf{R}\mathbf{x}\right\|^2 \leq C^2, \tag{2.16}$$

where $\mathbf{y}' = \mathbf{Q}^T\mathbf{y}$. If $N > M$, we will have

$$-C \leq y'_M - \left[r_{M,M}x_M + \cdots + r_{M,N}x_N\right] \leq C, \tag{2.17}$$

at the Mth layer. (2.17) involves N-M+1 dimensions for detection. (2.17) is similar to a detection problem of a real-valued MISO system. First, we want to find the constellation points falling inside this slab. There are two algorithms that can help us find those constellation points, i.e., Plane Decoding Algorithm and Slab Decoding Algorithm.

Plane Decoding Algorithm

For a MISO system with k transmitted antennas where the inputs are independent symbols, the received signal can be written as

$$y = h_1x_1 + \cdots + h_kx_k + \eta, \tag{2.18}$$

where $x_k \in \mathbb{Z}$, h_n is the channel response and $\eta \sim CN(0,\sigma^2)$ stands for AWGN. ML estimation of the transmitted vector $\mathbf{x} = [x_1,\cdots,x_k]$ can be written as

$$\mathbf{x}_{ML} = \arg\min_{(x_1,\cdots,x_k)\in\mathbb{Z}^k} \left(y - h_1x_1 + \cdots + h_kx_k\right)^2, \tag{2.19}$$

the estimator means to find the point $\mathbf{x} \in \mathbb{Z}^k$ which is the closest to the hyperplane P given as

$$P : h_1x_1 + \cdots + h_kx_k = y. \tag{2.20}$$

First, define X, X_V, X_{PD} as the sets of the points to be visited, the points that have been visited, and the points that are close to P in all dimensions, respectively. Then, initialize them with X= X_V = $\left\{\mathbf{x}^{(1)}\right\}$ where the (1) stands for the order of the vector in a set and $j = 1$.

The main idea of the PDA is to find those candidates (X_{PD}) which are close to P in all dimensions. The procedures of the PDA are summarized as follows:

Step 1: If X is empty, go to Step 5. Otherwise, we calculate

$$\hat{a}_j = \left\{ x : \min_{x \in \mathbb{Z}} x \text{ s.t. } x > x_B \right\}$$

$$\tilde{a}_j = \left\{ x : \max_{x \in \mathbb{Z}} x \text{ s.t. } x < x_B \right\},$$

where

$$x_B = x_j^{[1]} - \frac{\Delta y\left(\mathbf{x}^{(1)}\right)}{\left|h_j\right|}$$

$$\Delta y\left(\mathbf{x}^{(1)}\right) = \left|h_1\right| x_1^{[1]} + \left|h_2\right| x_2^{[1]} + \cdots + \left|h_k\right| x_k^{[1]} - y$$

Step 2: If $\{\hat{a}_k \neq \Phi\} \wedge \{\tilde{a}_k = \Phi\}$ is not true, go to Step 3. Otherwise, we have the point $\hat{\mathbf{x}} = \mathbf{x}^{(1)}$ except that $\hat{x}_j = \hat{a}_j$ where $\hat{\mathbf{x}}$ is close to P in dimension-j. Then, if $\hat{x}_j = x_j^{(1)}$ and then the point $\mathbf{x}^{(1)}$ is close to P in dimension-1,2,…,j and do:

- If $j < k$, update $j = j + 1$. Go to Step 1.
- If $j = k$, the point $\mathbf{x}^{(1)}$ is close to P in all dimensions and is stored in X_{PD}. Next, discard $\mathbf{x}^{(1)}$ from the set X and reset $j = 1$. Go back to Step 1 to check a new point in X.

Else, if $\hat{x}_j \neq a_j^{(1)}$, then discard $\mathbf{x}^{(1)}$ from the set X and reset $j = 1$. Go back to Step 1.

Step 3: If $\{\hat{a}_k = \Phi\} \wedge \{\tilde{a}_k \neq \Phi\}$ is not true, go to Step 4. Otherwise, we have the point $\tilde{\mathbf{x}} = \mathbf{x}^{(1)}$ except that $\tilde{x}_j = \tilde{a}_j$ where $\tilde{\mathbf{x}}$ is close to P in

dimension-j. Then, if $\tilde{x}_j = x_j^{(1)}$ and then the point $\mathbf{x}^{(1)}$ is close to P in dimension-1,2,…,j and do:

- If $j < k$, update $j = j + 1$. Go to Step 1.
- If $j = k$, the point $\mathbf{x}^{(1)}$ is close to P in all dimensions and is stored in X_{PD}. Next, discard $\mathbf{x}^{(1)}$ from the set X and reset $j = 1$. Go back to Step 1 to check a new point in X.

Else, if $\tilde{x}_j \neq a_j^{(1)}$, then discard $\mathbf{x}^{(1)}$ from the set X and reset $j = 1$. Go back to Step 1.

Step 4: If $\{\hat{a}_k \neq \Phi\} \wedge \{\tilde{a}_k \neq \Phi\}$ is not true, go to Step 5. Otherwise, we have two points $\hat{\mathbf{x}} = \mathbf{x}^{(1)}$ except that $\hat{x}_j = \hat{a}_j$ and $\tilde{\mathbf{x}} = \mathbf{x}^{(1)}$ except that $\tilde{x}_j = \tilde{a}_j$ where $\hat{\mathbf{x}}$ and $\tilde{\mathbf{x}}$ are close to P in dimension-j. Then, if $\hat{x}_j = x_j^{(1)}$ and then the point $\mathbf{x}^{(1)}$ is close to P in dimension-1,2,…,j and do:

- If $j < k$, update $j = j + 1$ and if $\tilde{\mathbf{x}} \notin X_V$ then update $X = \{X, \tilde{\mathbf{x}}\}$ and $X_V = \{X_V, \tilde{\mathbf{x}}\}$. Go to Step 1.
- If $j = k$, the point $\mathbf{x}^{(1)}$ is close to P in all dimensions and is stored in X_{PD}. Next, discard $\mathbf{x}^{(1)}$ from the set X and reset $j = 1$. Go back to Step 1 to check a new point in X.

If $\tilde{x}_j = x_j^{(1)}$ and then do:

- If $j < k$, update $j = j + 1$ and if $\hat{\mathbf{x}} \notin X_V$ then update $X = \{X, \hat{\mathbf{x}}\}$ and $X_V = \{X_V, \hat{\mathbf{x}}\}$. Go to Step 2.
- If $j = k$, the point $\mathbf{x}^{(1)}$ is close to P in all dimensions and is stored in

X_{PD}. Next, discard $\mathbf{x}^{(1)}$ from the set X and reset $j = 1$. Go back to Step 1 to check a new point in X.

Else, if $x_j^{(1)} \neq \hat{a}_j, \tilde{a}_j$, then discard $\mathbf{x}^{(1)}$ from the set X and reset $j = 1$. Go back to Step 1.

Step 5: Each point $\mathbf{x}$ in X_{PD}, update

$$x_k = -x_k \ \forall k \text{ if } h_k < 0.$$

The PDA guarantees to achieve the ML solution only for the MISO systems. For MIMO systems, we will need to find those points that fall inside the slab

$$-C \leq y - [h_1 x_1 + \cdots + h_k x_k] \leq C, \tag{2.21}$$

The following algorithm is designed to accomplish this.

Slab Decoding Algorithm

Obviously, although the X_{PD} does not contain all the lattice points that fall inside the slab in (2.21), the X_{PD} provides a useful starting point for slab detection.

The procedures of SDA are summarized as follows:

Step 1: Sorting the points of X_{PD} according to their Euclidean distances. Therefore,

$$X_{PD}^{\text{sort}} = \left\{\mathbf{x}_{PD}^{(1)}, \mathbf{x}_{PD}^{(2)}, \mathbf{x}_{PD}^{(3)}, \cdots\right\}$$

where $\Delta y^2\left(\mathbf{x}_{PD}^{(i)}\right) \leq \Delta y^2\left(\mathbf{x}_{PD}^{(j)}\right)$ if $i \leq j$.

Step 2: For a given C, find the set

$$X_{PD;\leq C^2} = \left\{\mathbf{x} \in X_{PD}^{\text{sort}} : -C \leq \Delta y(\mathbf{x}) \leq C\right\}$$

Step 3: For each point $\mathbf{x} \in X_{PD;\leq C^2}$, move away along each direction for

finding other points which $\Delta y^2(\mathbf{x}) \le C^2$. These newly found points are then added to $X_{PD;\le C^2}$. It is done by the following loop.

a. Initialize $n = 1$, and $j = 1$. Pick the nth point $\mathbf{u}^{(n)} \in X_{PD;\le C^2}$.

b. Compute

$$u_0 = \min\left(u_j^{(n)} + d, \max_{s\in\mathbb{Z}} s\right),$$

where d stands for the separation of every adjacent constellation.

If $u_j^{(n)} \neq u_0$ and then do the following.

- Set $u_j^{(n)} = u_0$.
- If $\Delta y^2\left(\mathbf{u}^{(n)}\right) \le C^2$, then $X_{PD;\le C^2} = \left\{X_{PD;\le C^2}, \mathbf{u}^{(n)}\right\}$.

c. Compute

$$u_0 = \max\left(u_j^{(n)} + d, \min_{s\in\mathbb{Z}} s\right).$$

If $u_j^{(n)} \neq u_0$ and then do the following.

- Set $u_j^{(n)} = u_0$.
- If $\Delta y^2\left(\mathbf{u}^{(n)}\right) \le C^2$, then $X_{PD;\le C^2} = \left\{X_{PD;\le C^2}, \mathbf{u}^{(n)}\right\}$.

d. If $j < k$, then update $j = j + 1$ and go back to b.

e. If $j = k$, then update $n = n + 1$ and $j = 1$. Then, go back to b.

f. If $n = \left|X_{PD;\le C^2}\right|$, then all lattice points that fall inside the slab are found.

The two algorithms can find all the lattice points satisfying (2.21) for a given *C*. Each point of the set can be substituted into the original problem in (2.16), to obtain

$$\left\|\mathbf{y}_G - \mathbf{R}_1\mathbf{x}_G\right\|^2 \le C^2 \tag{2.22}$$

where $\mathbf{y}_G \in \mathbb{R}^{M-1}$, $\mathbf{R}_1 \in \mathbb{R}^{M-1\times M-1}$ corresponds to the first $M-1$ columns and rows of the $\mathbf{R}$ and $\mathbf{x}_G = [x_1, x_2, \cdots, x_{M-1}] \in \mathbb{R}^{M-1}$. Since $\mathbf{R}_1$ is an upper triangular matrix with full rank, we can solve the problem by SDA directly. After the substitution of all points, the ML solution can be found.

2.5.3 Regularization Method

Regularization method intends to transfer the underdetermined MIMO systems to overdetermined MIMO systems. By doing this transformation, one can directly use the SDA in a simple way. It first considers a constant modulus constellation, and derives the algorithm. Then it shows how MIMO systems with non-constant modulus constellations can be adapted so that the algorithm is applicable. The ML detection is equivalent to

$$\min_{\mathbf{x}\in\mathbb{Z}^N} \|\mathbf{y}-\mathbf{H}\mathbf{x}\|^2 = \min_{\mathbf{x}\in\mathbb{Z}^N} \|\mathbf{R}(\rho-\mathbf{x})\|^2, \tag{2.23}$$

where $\mathbf{R}$ is an upper triangular matrix such that $\mathbf{R}^T\mathbf{R} = \mathbf{H}^T\mathbf{H}$. In the overdetermined MIMO systems, i.e. $M > N$, $\mathbf{H}^T\mathbf{H}$ is full rank. The SDA is applicable due to the non-zero diagonal terms of $\mathbf{R}$. However, for the underdetermined MIMO systems, i.e. $M < N$, the Cholesky factor $\mathbf{R}$ of $\mathbf{H}^H\mathbf{H}$ is rank-deficient and only the first *M* rows of $\mathbf{R}$ are non-zero. Because the elements of $\mathbf{x}$ are of constant modulus, that means the product $\alpha\mathbf{x}^T\mathbf{x}$ is a constant. We can get an equivalent minimization problem as

$$\begin{aligned}&\min_{\mathbf{x}\in S}\left(\|\mathbf{y}-\mathbf{H}\mathbf{x}\|^2 + \alpha\|\mathbf{x}\|^2\right)\\ &= \min_{\mathbf{x}\in S}\left[\mathbf{y}^H\mathbf{y} - \mathbf{y}^H\mathbf{H}\mathbf{x} - \mathbf{x}^H\mathbf{H}^H\mathbf{y} + \mathbf{x}^H\left(\mathbf{H}^H\mathbf{H}+\alpha\mathbf{I}_N\right)\mathbf{x}\right].\end{aligned} \tag{2.24}$$

Thus the matrix $\mathbf{G} = \mathbf{H}^H\mathbf{H} + \alpha\mathbf{I}_N$ is full rank. It can be Cholesky factorized as

$\mathbf{G} = \mathbf{D}^T\mathbf{D}$, and $\mathbf{D}$ is an upper triangular matrix. By defining $\boldsymbol{\lambda} = \mathbf{G}^{-1}\mathbf{H}^H\mathbf{y}$, (2.24) is equivalent to

$$\min_{\mathbf{x}\in S} \left\|\mathbf{D}(\boldsymbol{\lambda} - \mathbf{X})\right\|^2. \tag{2.25}$$

(2.25) is an overdetermined case, thus can directly use SDA. If the constellation is not constant modulus, the non-constant modulus constellation can be represented as combination of constant modulus constellations. For example, *q*-QAM ($q = 2^k$) can be represented as a weighted sum of $k/2$ QPSK constellations when *k* is an even number. That is, for $w \in$q-QAM and $w_i \in$QPSK, $0 \le i < k/2$, we have

$$z = \sum_{i=0}^{\frac{k}{2}-1} 2^i \left(\frac{\sqrt{2}}{2}\right) z_i .$$

2.6 Summary

In this chapter, we give a review of the MIMO communication systems. Exploiting multi-path scattering, MIMO systems deliver significant performance enhancements in terms of data rate and link quality. Spatial diversity is one of the MIMO techniques which mitigates fading and is realized by providing the receiver with multiple copies of the transmitted signal in space or time. MIMO systems offer a linear increase in data rate through spatial multiplexing by transmitting multiple and independent data streams without requiring additional bandwidth or transmit power. The underdetermined MIMO systems can be solved by several algorithms. GSD algorithm has to perform exhaustive search over ($N-M$) dimensions. The SSD checks all the points in a geometrical slab. The regularization method transfer the underdetermined case to overdetermined one by adding a constant term.

Chapter 3

Proposed Transmit Power Allocation

In this chapter, we introduce the proposed transmit power allocation for MU-MIMO systems. We aim to find a power allocation matrix such that all user data rate will be close to each other. We choose the sum of logarithmic average user rates as our utility function. We reformulate this nonlinear optimization problem to a suitable form, thus the Interior-point method can be applied. The proposed method can also be applied to single user MIMO (SU-MIMO) systems. The simulation results shows that the proposed method provides fair data rate for all users. The Chapter is organized as follows. In Section 3.1, we introduce that the special uplink MU-MIMO can be regarded as the underdetermined MIMO system. The proposed transmit power allocation is introduced in Section 3.2. The reformulation of the nonlinear optimization problem and Interior-point algorithm are described in Section 3.3. Section 3.4 contains the numerical results of the proposed method, and Section 3.5 summarizes this chapter.

3.1 Uplink MU-MIMO System

In the uplink scenario, if there are *N* users transmit the signal simultaneously, and each user is equipped with one antenna. The base station has *M* antennas. When the number of base station antennas *M* is larger than the number of users *N*, it can be viewed as an underdetermined MIMO system. Therefore, the existing algorithms can be used to decode the received signals. Fig. 3.1 is a practical example in uplink MU-MIMO system. User 6 is blocked by a high building and User 11 is far away from the base station. The channel gains are depending on the shadowing and distance between the transmitter and receiver. In general, these two users will suffer from small channel gains. Hence, User 6 and 11 will have lower data rates than the other users. We aim to use a power allocation to let all users have fair rates. Thus User 6 and User 11 will achieve higher data rates.

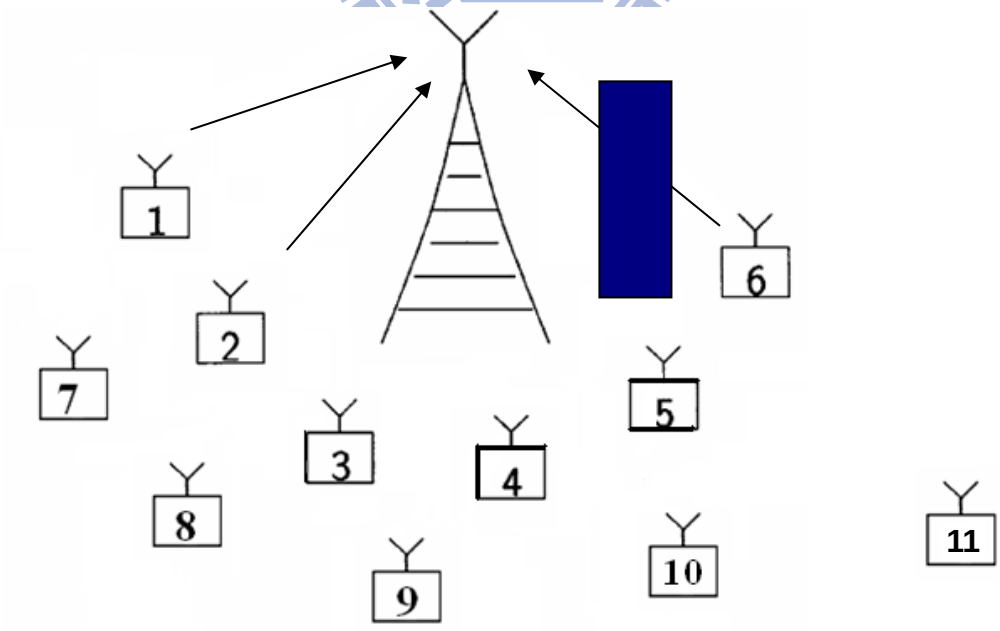

Fig. 3-1 Example of uplink MU-MIMO system.

3.2 Proposed Transmit Power Allocation for Fair Rates

In the uplink MU-MIMO systems, the users are independent and separated. They cannot exchange the information to each other. Thus precoding techniques at the transmitter cannot be applied in this case. However, we can use power allocation to improve the performance. The transmit power allocation is proposed to allocate power to different users. We incorporate the power allocation matrix $\mathbf{P} = diag\left(\sqrt{P_1}, \sqrt{P_2}, \cdots, \sqrt{P_N}\right)$ into our system model, where P_i is the power transmitted by the ith user. Thus, the received signal in (2.3) becomes

$$\mathbf{y} = \mathbf{HPx} + \mathbf{n}, \tag{3.1}$$

and $P_i \le P_{\max i}$ is the power constraint for the ith user. The matrix $\mathbf{HP}$ in (3.1) can be regarded as the equivalent channel matrix. It can also be considered as matrix $\mathbf{P}$ provides different gains to different columns of $\mathbf{H}$. Assuming that the receiver has the perfect channel state information (CSI). The maximum achievable rate for the ith user is

$$R_i = \log_2(1 + \mathrm{SINR}_i), \qquad i = 1, 2, \cdots, N \tag{3.2}$$

where $\mathrm{SINR}_i = \dfrac{\left(|h_{1i}|^2 + |h_{2i}|^2 + \cdots + |h_{Mi}|^2\right) P_i}{M\sigma^2 + \sum_{j \ne i} \left(|h_{1j}|^2 + |h_{2j}|^2 + \cdots + |h_{Mj}|^2\right) P_j}$ and σ^2 is the noise power. Here we treat the other users as interference at the receiver. By the concept of [21], we choose the utility function $U\left(R_1, R_2, \cdots, R_N\right)$ as

$$U_{\mathrm{F}}\left(R_1, R_2, \cdots, R_N\right) = \ln\left(R_1\right) + \ln\left(R_2\right) + \cdots + \ln\left(R_N\right). \tag{3.3}$$

We want to find the matrix $\mathbf{P}^*$ which maximizes the utility function. This lead to the

following optimization problem:

$$\max \; U_{\mathrm{F}}\left(R_1, R_2, \cdots, R_N\right) \qquad \text{subject to} \;\; P_i \le P_{\max i} \quad i = 1, 2, \cdots, N \qquad (3.4)$$

We choose the logarithm function in (3.3) because it provides better fairness for the rate R_i of each user. For logarithm function, the larger input, the more suppressed output. This means that the different rates will be closer to each other. If we choose the utility function as $U_{\mathrm{sum}}\left(R_1, R_2, \cdots, R_N\right) = R_1 + R_2 + \cdots + R_N$, i.e., maximizing the total sum rate, then the water filling algorithm [18] will be the solution.

The utility function in (3.3) can also be applied to SU-MIMO system. The difference between SU-MIMO and MU-MIMO systems is the power constraint. When the transmitter has *N* antennas and receiver has *M* antennas, the received signal can be written as same as (3.1). The optimization problem in (3.4) becomes

$$\max \; U_{\mathrm{F}}\left(R_1, R_2, \cdots, R_N\right) \qquad \text{subject to} \qquad \sum_{i=1}^{N} P_i \le P_{\mathrm{max}} .$$

where P_i is the transmitted power of the ith antenna and P_{max} is the maximum transmit power. The achievable data rate will become fair for all users with the proposed power allocation applied.

In [26] we know that the optimization problem in (3.4) cannot be solve mathematically as a closed form. The reason is that the utility function is a very complicated nonlinear function. Thus we need to reformulate the problem to a suitable form which can be solved by the existing algorithms. Here we choose the interior-point method [23], [24] to solve the optimization problem, since it is more efficient and applicable to both linear and nonlinear problems.

3.3 Interior Point Algorithm

In this Section, we reformulate the optimization problem in (3.4) to apply the existing algorithms. We start from transforming our optimization problem to a suitable form for the Interior-point method, and then give a brief algorithm of the Interior-point method. We can regard (3.4) as the constrained nonlinear optimization problem:

$$\min \quad f(\mathbf{x}) \qquad \text{subject to} \quad c_j(\mathbf{x}) \geq 0, \quad j = 1,2,\cdots,N$$

where $f(\mathbf{x}) = -U_{\mathrm{F}}\left(R_1, R_2, \cdots, R_N\right)$ and $c_j(\mathbf{x}) = -P_j + P_{\max j}$ are continuous and have continuous second partial derivatives. By introducing the slack variable $\mathbf{y} = [y_1, y_2, \cdots, y_N]$, the problem can be converted to

$$\min \quad f(\mathbf{x}) \qquad \text{subject to} \quad \mathbf{c}(\mathbf{x}) - \mathbf{y} = 0, \quad \mathbf{y} \geq \mathbf{0}$$

where $\mathbf{c}(\mathbf{x}) = [c_1(\mathbf{x}), c_2(\mathbf{x}), \cdots, c_N(\mathbf{x})]^T$. The inequality constraint $\mathbf{y} \geq \mathbf{0}$ can be incorporated into the objective function by adding a logarithmic barrier function. This yields the minimization problem :

$$\min \quad f_\tau(\mathbf{x}) = f(\mathbf{x}) - \tau \sum_{i=1}^{N} \ln y_i \quad \text{subject to} \quad \mathbf{c}(\mathbf{x}) - \mathbf{y} = 0 \qquad (3.5)$$

where $\tau > 0$ is the barrier parameter. Hence all the constraints are equalities. The term $-\tau \sum_{i=1}^{N} \ln y_i$ in (3.5) acts like a barrier that prevents any component y_i from becoming negative, since the logarithm function has no definition on the negative values. We solve the problem (3.5), and obtain the optimal solution to the original problem as $\tau \to 0$. The Lagrangian for the problem in (3.5) is

$$\mathrm{L}(\mathbf{x}, \mathbf{y}, \boldsymbol{\lambda}, \tau) = f(\mathbf{x}) - \tau \sum_{i=1}^{N} \ln y_i - \boldsymbol{\lambda}^T [\mathbf{c}(\mathbf{x}) - \mathbf{y}] \qquad (3.6)$$

and the KKT conditions for the problem in (3.4) are given by

$$\nabla_x \mathrm{L} = \nabla f(\mathbf{x}) - \mathbf{A}^T(\mathbf{x})\boldsymbol{\lambda} = 0,$$

$$\nabla_y \mathrm{L} = -\tau \mathbf{Y}^{-1}\mathbf{e} + \boldsymbol{\lambda} = 0,$$

$$\nabla_{\boldsymbol{\lambda}} \mathrm{L} = \mathbf{c}(\mathbf{x}) - \mathbf{y} = 0,$$

where

$$\mathbf{A}(\mathbf{x}) = \left[\nabla c_1(\mathbf{x}), \nabla c_2(\mathbf{x}), \cdots, \nabla c_N(\mathbf{x})\right]^T$$

$$\mathbf{Y} = \mathrm{diag}\left\{y_1, y_2, \cdots, y_N\right\}$$

$$\mathbf{e} = [1,1,\cdots,1]^T.$$

Once we reformulate the optimization problem in (3.4) to the form of (3.5), the problem can be applied to Interior-point algorithm by using the Lagrangian function in (3.6).

The interior-point algorithm can be briefly summarized as follows.

Step 1. Input an initial set $\left\{\mathbf{x_0}, \mathbf{y_0}, \boldsymbol{\lambda}_0\right\}$ with $\mathbf{y_0} > 0$, $\boldsymbol{\lambda}_0 > 0$, and an intitial barrier parameter τ_0. Set $l = 0$, $\left\{\mathbf{x}_0^*, \mathbf{y}_0^*, \boldsymbol{\lambda}_0^*\right\} = \left\{\mathbf{x_0}, \mathbf{y_0}, \boldsymbol{\lambda}_0\right\}$, and initialize the outer-loop tolerance $\varepsilon_{\text{outer}}$.

Step 2. Set $k = 0$, $\tau = \tau_l$, and initialize the inner-loop tolerance $\varepsilon_{\text{inner}}$.

Step 3. Using the first and second derivatives to evaluate $\left\{\Delta\mathbf{x}_k, \Delta\mathbf{y}_k, \Delta\boldsymbol{\lambda}_{\mathrm{k}}\right\}$ and α_k such that $\begin{cases} \mathbf{x}_{k+1} = \mathbf{x}_k + \alpha_k \Delta\mathbf{x}_k \\ \mathbf{y}_{k+1} = \mathbf{y}_k + \alpha_k \Delta\mathbf{y}_k \\ \boldsymbol{\lambda}_{\mathrm{k+1}} = \boldsymbol{\lambda}_{\mathrm{k}} + \alpha_k \Delta\boldsymbol{\lambda}_{\mathrm{k}} \end{cases}$ will get a descent direction for the objective function.

Step 4. If $\left\|\alpha_k \Delta\mathbf{x}_k\right\| + \left\|\alpha_k \Delta\mathbf{y}_k\right\| + \left\|\alpha_k \Delta\boldsymbol{\lambda}_{\mathrm{k}}\right\| < \varepsilon_{\text{inner}}$,

set $\left\{\mathbf{x}_{l+1}^*, \mathbf{y}_{l+1}^*, \boldsymbol{\lambda}_{l+1}^*\right\} = \left\{\mathbf{x}_{k+1}, \mathbf{y}_{k+1}, \boldsymbol{\lambda}_{k+1}\right\}$ and continue to Step 5;

otherwise, set $k = k+1$ and repeat from step 3.

Step 5. If $\left\|\mathbf{x}_l^* - \mathbf{x}_{l+1}^*\right\| + \left\|\mathbf{y}_l^* - \mathbf{y}_{l+1}^*\right\| + \left\|\boldsymbol{\lambda}_l^* - \boldsymbol{\lambda}_{l+1}^*\right\| < \varepsilon_{\text{outer}}$, output

$\left\{\mathbf{x}^*, \mathbf{y}^*, \boldsymbol{\lambda}^*\right\} = \left\{\mathbf{x}_l^*, \mathbf{y}_l^*, \boldsymbol{\lambda}_l^*\right\}$ and stop; otherwise, calculate τ_{l+1}, set

$\left\{\mathbf{x_0}, \mathbf{y_0}, \boldsymbol{\lambda}_0\right\} = \left\{\mathbf{x}_l^*, \mathbf{y}_l^*, \boldsymbol{\lambda}_l^*\right\}$, $l = l + 1$, and repeat from Step 2.

The Interior-point algorithm is described by two loops. The two loops can prevent finding the local minimum. This algorithm will be convergent by choosing appropriate error tolerances.

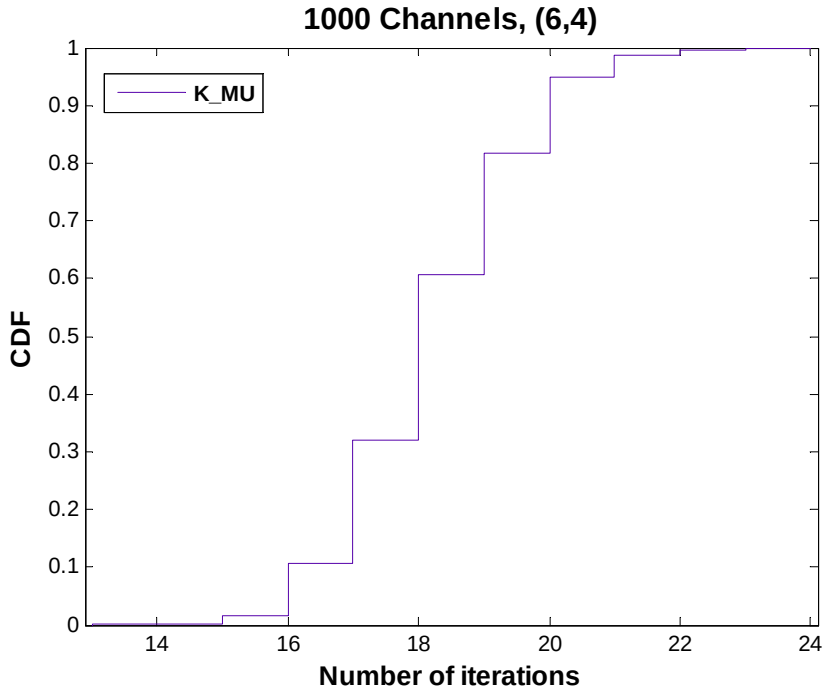

Fig. 3-2 CDF of the number of iterations for interior-point algorithm

Fig. 3-2 is the CDF as a function of the number of iterations when the interior-point algorithm is applied to solve our optimization problem. There are 1000 channel realizations and $M = 4$, $N = 6$. We choose the error tolerances to be 0.1. Fig. 3-2 shows that the range of the number of iterations is between 15 and 22. After solving the optimization problem in (3.3), we obtain the optimal $\mathbf{P}^*$ such that the different rates R_i will be closer to each other.

3.4 Computer Simulations

In this section, we simulate the proposed power allocation for MU-MIMO systems. All the simulations are measured and averaged over 1000 independent channels. Here $M = 4$ and $N = 6$. Fig. 3-3 shows the PDF of the ratio of minimum rate to maximum rate. We can see that the ratio tend to approach to 1. That also means the proposed power allocation will tend to uniform data rates.

Fig. 3-4 simulates the minimum user data rates versus the reciprocal of channel gains in 1000 channel realizations. It compares the three schemes: waterfilling power allocation, no power allocation, and the proposed fairness power allocation. Since the channel gain

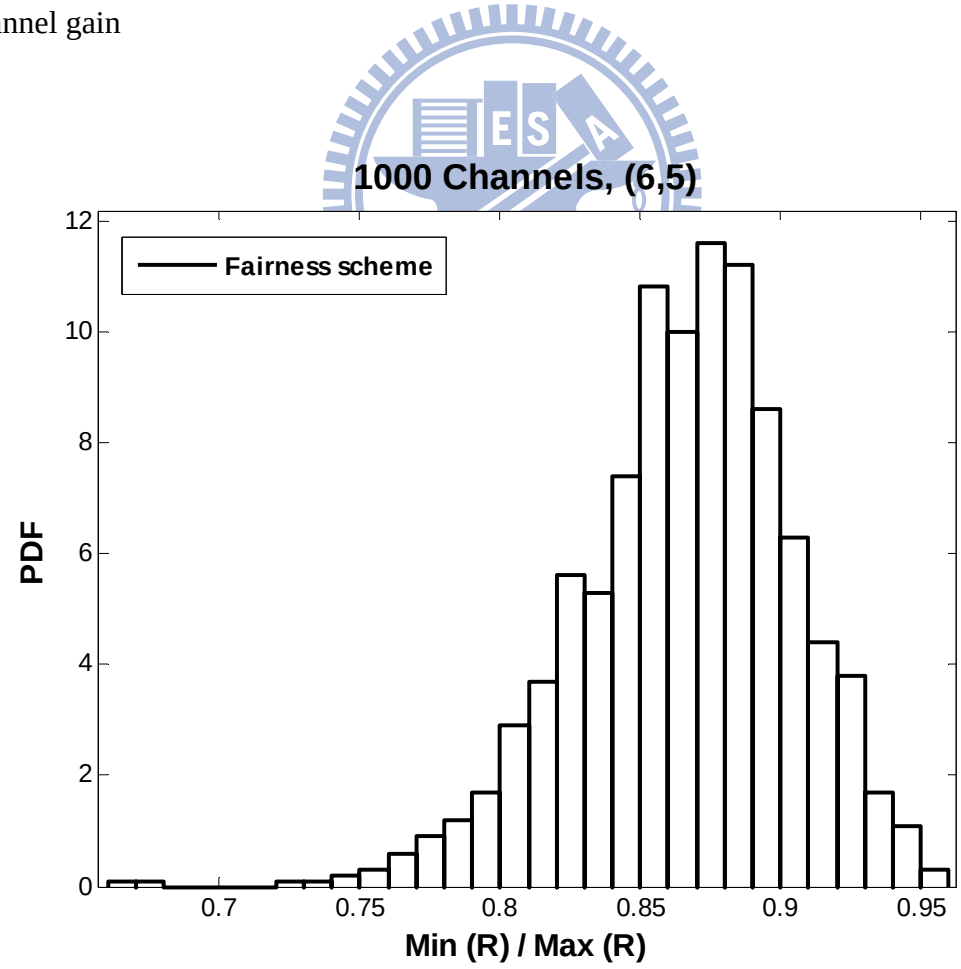

Fig. 3-3 The PDF of the ratio of minimum rate to maximum rate

is inversely proportional to the square of distance between the transmitter and receiver, the horizontal axis can be regarded as the user's distance from the base station. In the waterfilling power allocation scheme, the user may be turned off when the distance is large enough. If we choose the fairness power allocation scheme, the smallest user rate will be larger than the other two schemes. Fig. 3-5 simulates the maximum user rates versus the reciprocal of channel gains in 1000 channel realizations. In the waterfilling power allocation scheme, the user with best channel gain will be allocated with the largest power, thus the achieved rates will be higher than the other schemes. In the fairness power allocation scheme, we sacrifice the rate of the best user and obtain more fair rates.

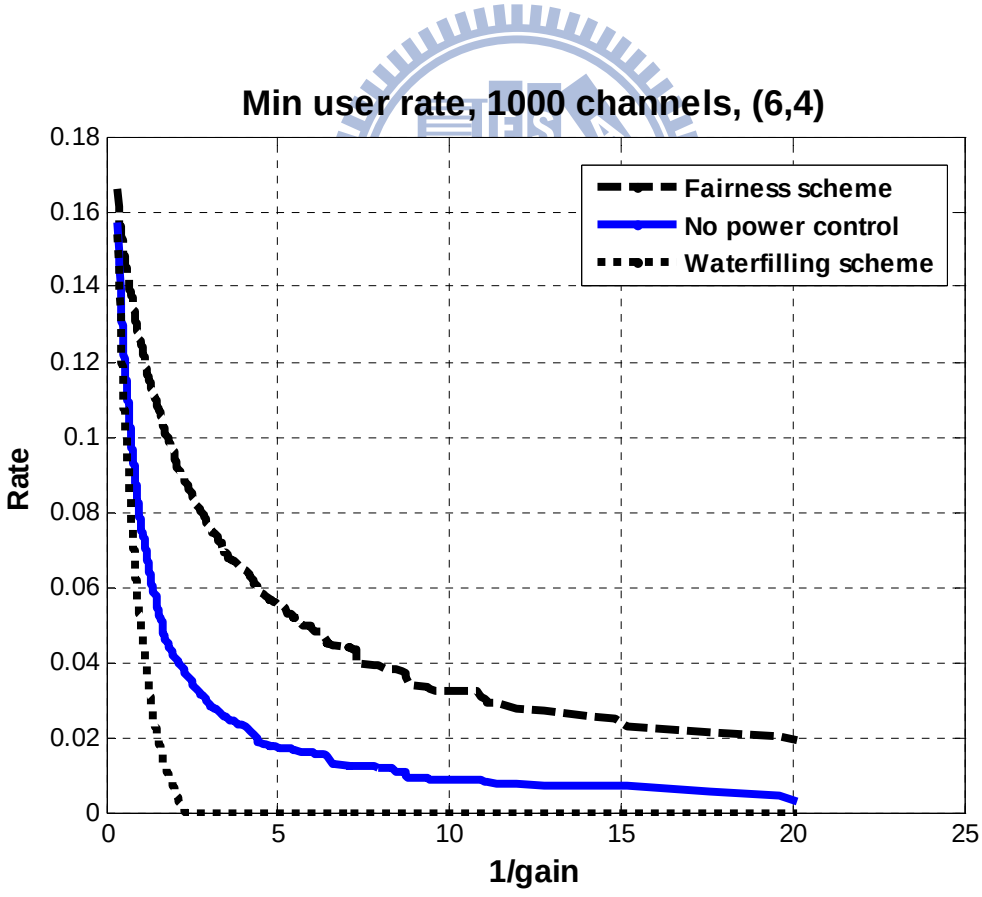

Fig. 3-4 Minimum rates versus reciprocal of channel gains

Fig. 3-6 compares the sum rate of four users with different schemes. In the waterfilling power allocation scheme, the utility function is chosen to maximize the sum rate of all users. Thus, the sum rate of the waterfilling scheme is always higher than the other schemes. Although the sum rate of the proposed fairness scheme is lower than the scheme without power allocation, it could obtain fair rates for all users.

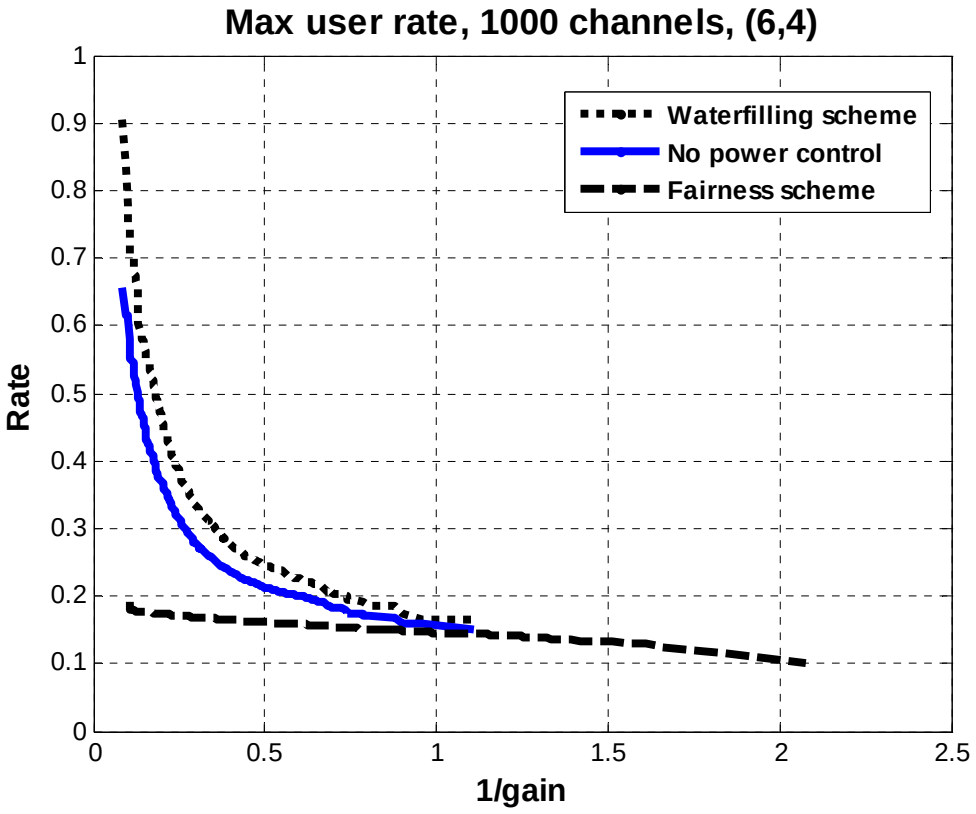

Fig. 3-5 Maximum rates versus reciprocal of channel gains

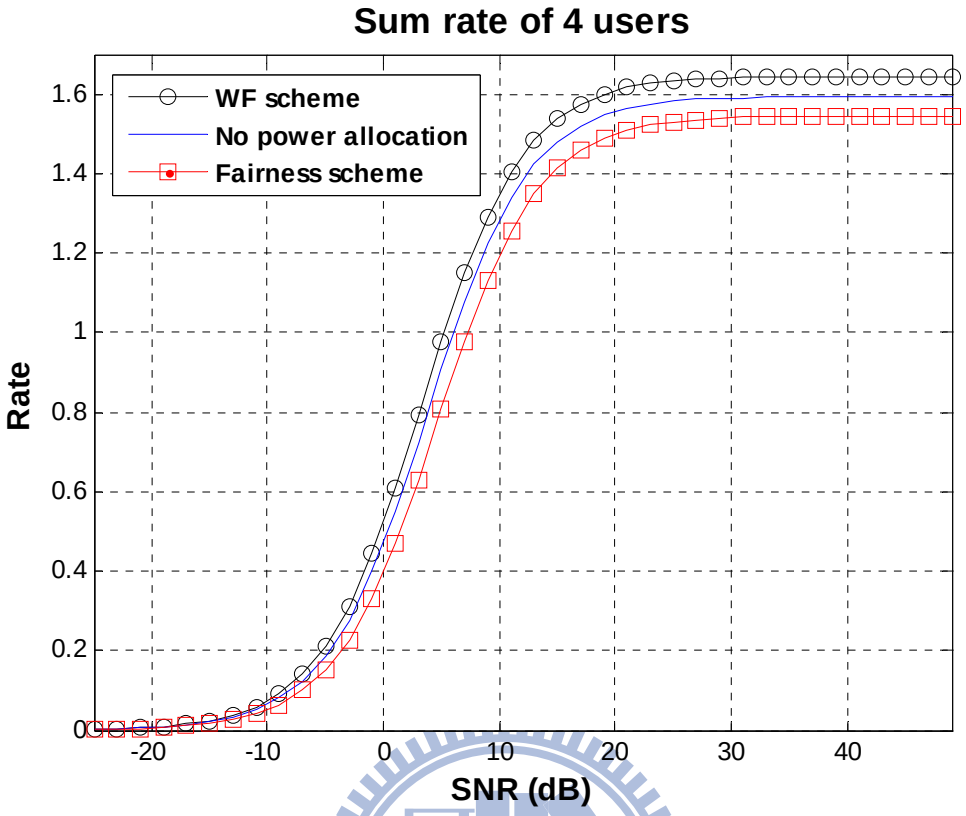

Fig. 3-6 Sum rate comparison for fairness scheme

3.5 Summary

In this chapter we give a detailed description of the proposed transmit power allocation. We reformulate the nonlinear optimization problem, and apply the Interior-point method to solve it. In both SU-MIMO and MU-MIMO systems, after the proposed transmit power allocation, all users will tend to have fair transmission rates. This means that it can prevent the users with small channel gains from suffering poor data rates. We compare the sum rate of the waterfilling power allocation and the scheme without power allocation with the proposed power allocation. It's a trade-off between the maximum average throughput and user fairness.

Chapter 4

Condition Number Discussion

In Chapter 3, we have introduced the proposed transmit power allocation with proportional fairness rates. This means that the sub-channel gains will be close to each other with the proposed power allocation applied. And the equivalent channel matrix will tend to be a well-conditioned channel matrix. In this chapter, we state that the condition number of the equivalent channel matrix is statistically smaller by observing the simulation results. If an underdetermined MIMO system is well-conditioned, the decoding complexity of the executed SDA will be reduced. Motivated by the fairness scheme, we propose a determinant based power allocation to further reduce the condition number of the equivalent matrix. Thus the decoding complexity of the underdetermined systems can be reduced with the proposed power allocation applied. In Section 4.1, we explain why the decoding complexity can be reduced with a smaller condition number. The determinant based utility function is provided in Section 4.2. Section 4.3 shows the simulation results. Section 4.4 summarizes this chapter.

4.1 Condition Number Effect

Although SDA can reduce the decoding complexity of ML detection from exponentially increasing to polynomially increasing, its complexity still grows heavily when the condition number of the channel matrix is large. The condition number is traditionally and calculated by taking the ratio of the maximum to minimum singular values of the channel matrix. For MIMO systems, the channel condition number is calculated from the instantaneous channel matrix without the need for stochastic averaging. Small values for the condition number imply a well-conditioned channel matrix while large values indicate an ill-conditioned channel matrix.

Consider an overdetermined MIMO systems with N transmit antennas and M receive antennas. The idea of SDA is to check all the points in a hyper-sphere with radius d. It finds the nearest point from the received signal to be the estimated signal. That is,

$$\hat{\mathbf{x}} = \arg\min_{\mathbf{x}\in\mathbb{Z}^N} \|\mathbf{y}-\mathbf{H}\mathbf{x}\|^2 = \arg\min_{\mathbf{x}\in\mathbb{Z}^N} \|\overline{\mathbf{y}}-\mathbf{R}\mathbf{x}\|^2 < d^2, \tag{4.1}$$

where $\mathbf{H}=\mathbf{Q}\mathbf{R}$, $\overline{\mathbf{y}}=\mathbf{Q}^T\mathbf{y}$, and $\mathbf{R}$ is the upper triangular matrix. Without loss of generality, we let $N=M$. We can rewrite (4.1) as a summation form $\sum_{i=1}^{M}\left(\overline{y}_i-\sum_{j=i}^{N} r_{ij}x_j\right)^2 < d^2$, start from the last equation and work backward. We expand the last equation as

$$\frac{\overline{y}_N - d}{r_{NN}} < x_N < \frac{\overline{y}_N + d}{r_{NN}}. \tag{4.2}$$

It means that all the constellation points satisfy (4.2) could be the candidate of x_N. The *i*th element of $\mathbf{x}$ will be bounded by

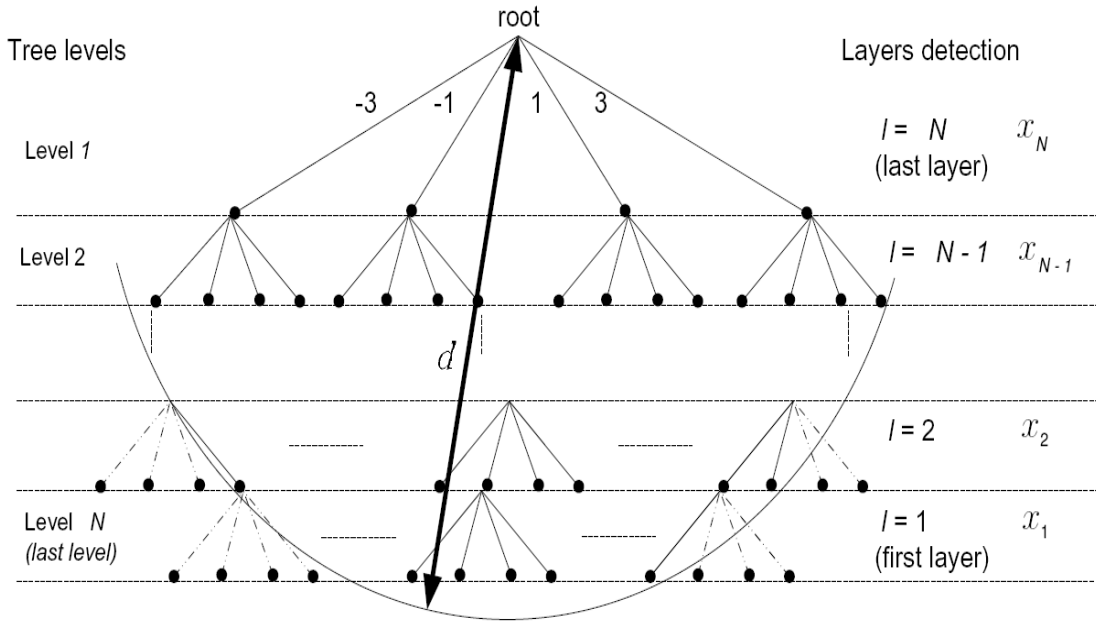

Fig. 4-1 Tree search example for 4-PAM showing sphere radius, tree levels and detection layers

$$\frac{\bar{y}_i - d - \sum_{j=i+1}^{N} r_{ij}x_j}{r_{ii}} < x_i < \frac{\bar{y}_i + d - \sum_{j=i+1}^{N} r_{ij}x_j}{r_{ii}}. \tag{4.3}$$

From (4.2) and (4.3), we know that SDA is a tree search. Fig. 4-1 is a tree search example for the 4-PAM constellation. We can search from Level 1 to Level N, and the distance for all levels should be less than the radius d. Because SDA decodes the transmit signal from the last layer x_N, the boundary of x_N should be as small as possible. This will reduce the number of searching points, as well as the decoding complexity.

In [22], we know that the r_{NN} of $\mathbf{R}$ depends on the condition number of the channel matrix $\mathbf{H}$. The lower the condition number is, the larger the r_{NN} is. Thus, we can obtain a lower decoding complexity when the system is well-conditioned. Fig. 4-2 shows the CDF of r_{55} for a 5×5 matrix with different condition numbers. We can see that when the condition number is less than 10, the value of r_{55} will tend

to be larger. Fig. 4-3 shows the FLOPS (Floating Point Operation Per Second) of the

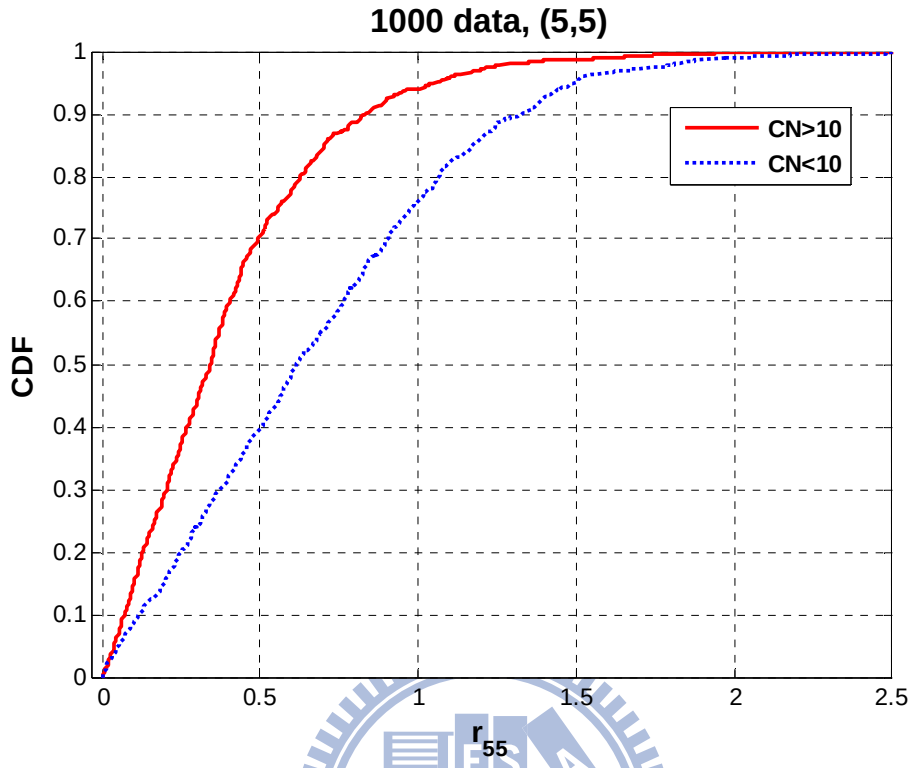

Fig. 4-2 CDF of r_{55} for a 5×5 matrix with different condition numbers

SDA versus condition number. The transmitter and receiver are both equipped with four antennas, and the transmitter uses the QPSK modulation. We can see that when the condition number is larger than 5 the complexity increase rapidly. Fig. 4-4 shows the CDF (Cumulative Density Function) of the condition number with different channel correlation. Assuming that there are 1000 channel realizations in a 2×2 MIMO system. Let $\mathbf{R}_{hh}$ be the correlation matrix of $\mathbf{H}$. A useful measure of the degradation in performance due to channel correlation, for a system with *K* diversity branches, is provided by the *K*th root of the determinant of the channel correlation matrix, $\det(\mathbf{R}_{hh})^{1/K}$ [24]. If $\det(\mathbf{R}_{hh})^{1/K}$ is smaller than 0.5, it can be regarded as high correlation. If $\det(\mathbf{R}_{hh})^{1/K}$ is larger than 0.5, it can be regarded as low correlation. Typically, we consider it to be an ill-conditioned channel when the

condition number is larger than 10 dB. Fig. 4-4 shows that both channels with low and high correlation are probable to be ill-conditioned channels. It also shows that a MIMO system is more likely to have a lower condition number when the channel has low correlation.

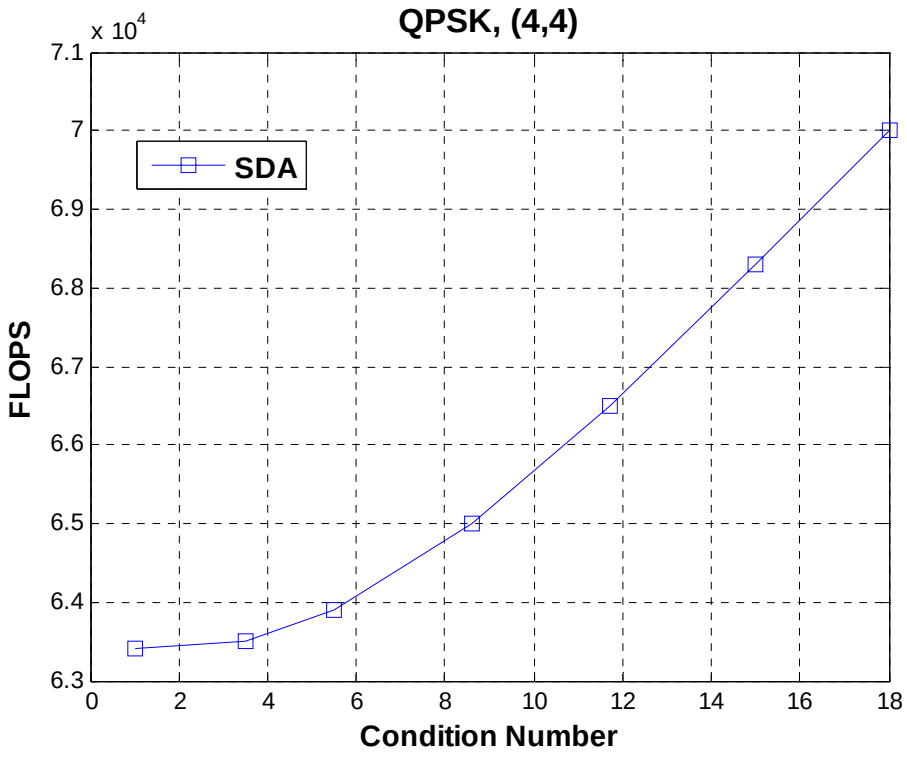

Fig. 4-3 Complexity as a function of condition number

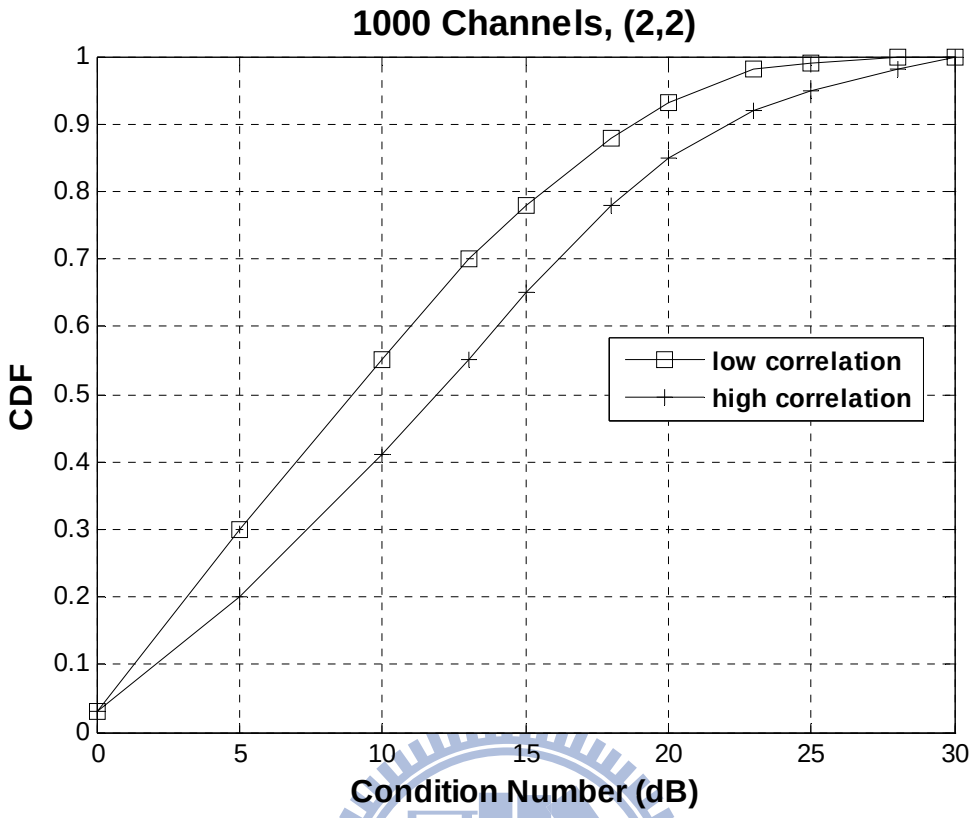

Fig. 4-4 CDF of condition number with different channel correlations

4.2 Proposed Utility Function for Condition Number

In Chapter 3, we know that the proposed transmit power allocation results in proportional fairness data rates. That means that the data rate for each user $R_i = \log_2(1 + \mathrm{SINR}_i)$ will be close to each other. The SINR in the log function will also be close to each other. When the data is transmitted from the *i*th user, the SINR at the receiver can be written as $\mathrm{SINR}_i = \dfrac{\|\mathbf{h}_i\|^2 P_i}{\mathrm{Noise} + \sum_{j \neq i} \|\mathbf{h}_j\|^2 P_j}$. $\mathbf{h}_i$ is the column vector of the channel matrix $\mathbf{H}$. At the high SNR, the data rate will be interference-limited. The sub-channel gain will be close to each other with the

proposed power allocation applied. That is,

$$\|\mathbf{h}_1\|^2 P_1 \approx \|\mathbf{h}_2\|^2 P_2 \approx \cdots \approx \|\mathbf{h}_N\|^2 P_N .$$

Thus the equivalent channel matrix will tend to be a well-conditioned channel matrix.

From the above concepts, we want to check if the condition number will be smaller with the proposed power allocation applied by computer simulations. We simulate the proposed transmit power allocation in the underdetermined SU-MIMO and MU-MIMO systems. Fig. 4-5 and Fig. 4-6 are the CDF as a function of the condition number. We simulate 1000 channel realizations, and the number of transmit and receive antennas are 6 and 4, respectively. Both SU-MIMO and MU-MIMO systems can obtain a smaller condition number with the proposed power allocation applied. By observing the simulation results, we can state that the condition number of the equivalent channel matrix is statistically smaller with the proposed power allocation applied.

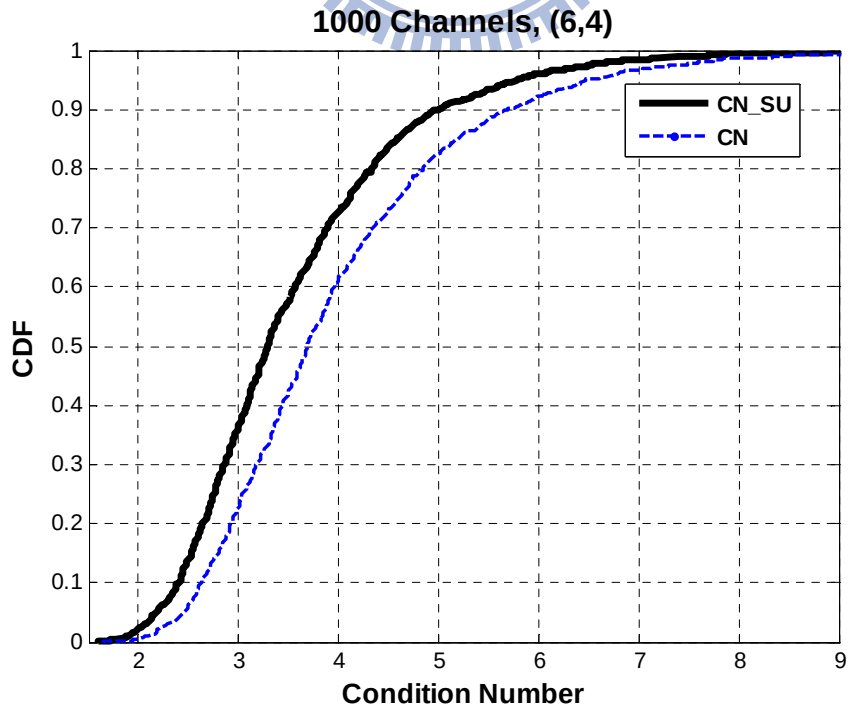

Fig. 4-5 CDF of the condition number for SU-MIMO

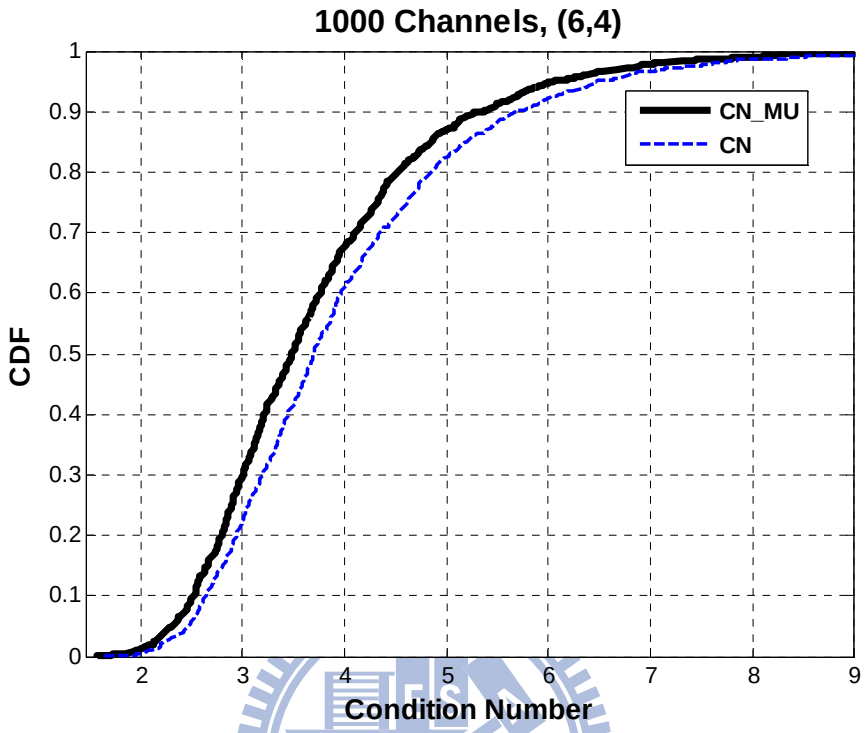

Fig. 4-6 CDF of the condition number for MU-MIMO

Motivated by the fairness scheme, we want to make the condition number of the equivalent channel matrix smaller. Thus the decoding complexity of the underdetermined MIMO systems can be reduced. From the linear algebra, we know that the determinant of a matrix is the products of all eigenvalues. For example, given a full rank 5×5 matrix $\mathbf{A}$, and $\lambda_1,\lambda_2,\cdots,\lambda_5$ are the eigenvalues of matrix $\mathbf{A}$. Then $\det(\mathbf{A})=\lambda_1\lambda_2\cdots\lambda_5$ and $\mathrm{trace}(\mathbf{A})=\lambda_1+\lambda_2+\cdots+\lambda_5$. Thus we propose a power allocation utility function based on the determinant to make the eigenvalues of the equivalent channel matrix close to each other. That will lead to smaller condition number. The optimization problem can be written as

$$\max\ \log\left(\det\left(HP(HP)^H\right)\right) \qquad \text{subject to} \qquad \mathrm{trace}\left(HP(HP)^H\right)=\text{constant}.$$

We use the techniques we've used in chapter 3 to reformulate the optimization

problem. And then we can apply the interior point algorithm to solve this. Fig. 4-7 is the comparison of condition number for fairness scheme and determinant based scheme. We simulate 1000 channel realizations, and the number of transmit and receive antennas are 6 and 5, respectively. It shows that both schemes can reduce the condition number statistically. The determinant based power allocation scheme leads to smaller condition number than the fairness scheme.

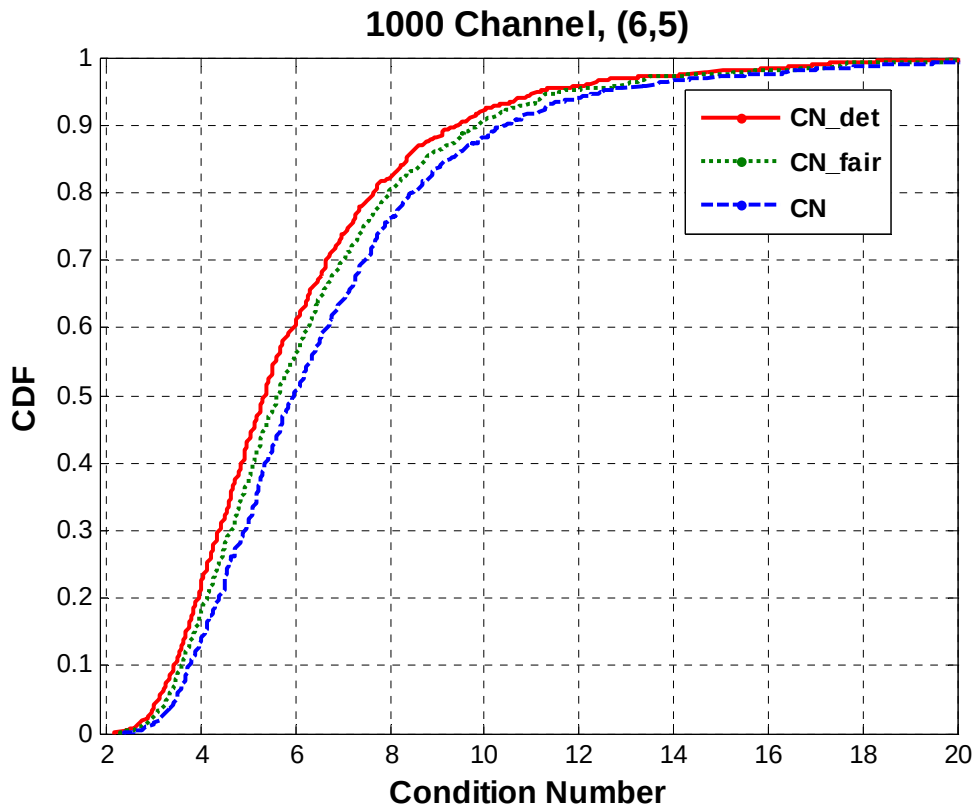

Fig. 4-7 Comparisons of condition number for fairness scheme and determinant based scheme

4.3 Computer Simulations

In this section, we simulate the decoding complexity of the SSD decoder and regularization decoder for underdetermined MIMO systems with the proposed power allocation applied. We also apply the proposed power allocation with the determinant based utility function to simulate the decoding complexity. Here the complexity weights of different operations is determined according to [16]. The numerical results are measured and averaged over 1000 independent channels for various average signal-to-noise ratio (SNR).

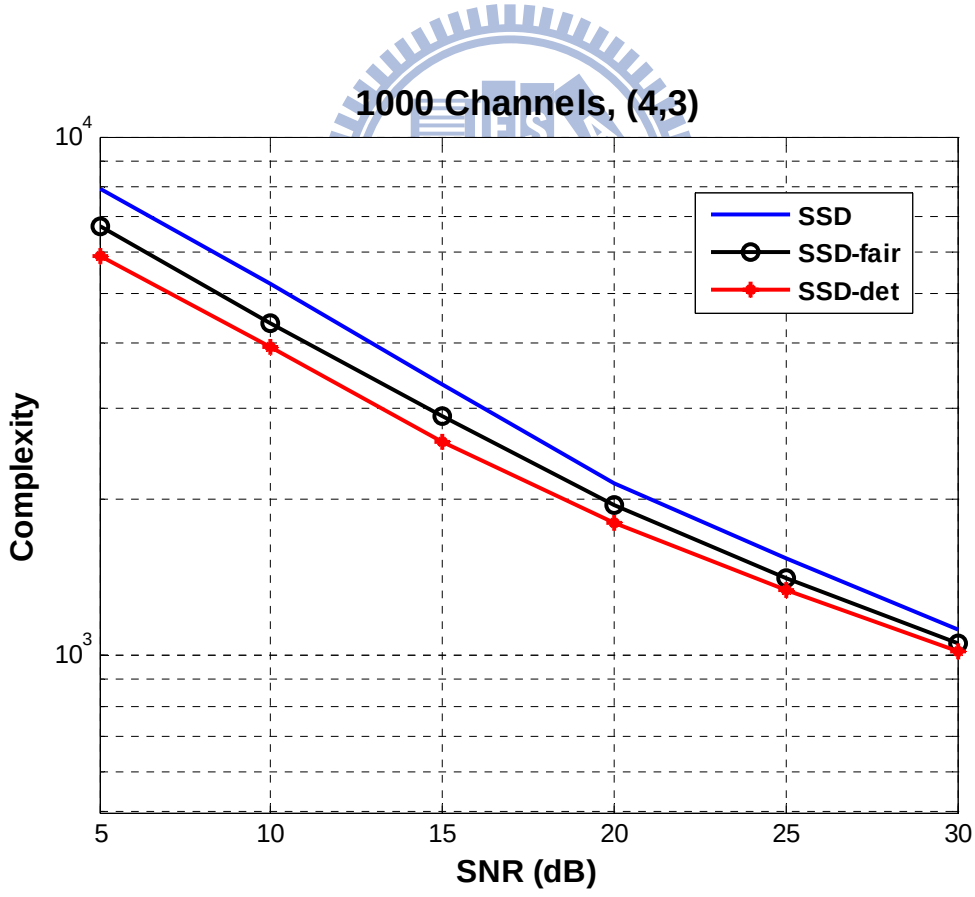

Fig. 4-8 Decoding complexity comparison using SSD at receiver. Transmitter has four antennas, and receiver has three antennas.

Fig. 4-8 shows the decoding complexity improvement with the proposed power allocations applied. In this simulation, we use 16-QAM modulation. The transmitter has four antennas and the receiver has three antennas. We choose the geometrical SSD to decode the underdetermined MIMO system. The SSD first finds the candidates in a slab and each candidate is followed by an SDA. Therefore, when the channel condition number is small, the decoding complexity can be reduced. Since the number of candidates in the slab depends on the noise, the larger the noise is, the more the candidate is. The SSD needs to activate more times of SDA at low SNR, thus the decoding complexity can be reduced more than at high SNR.

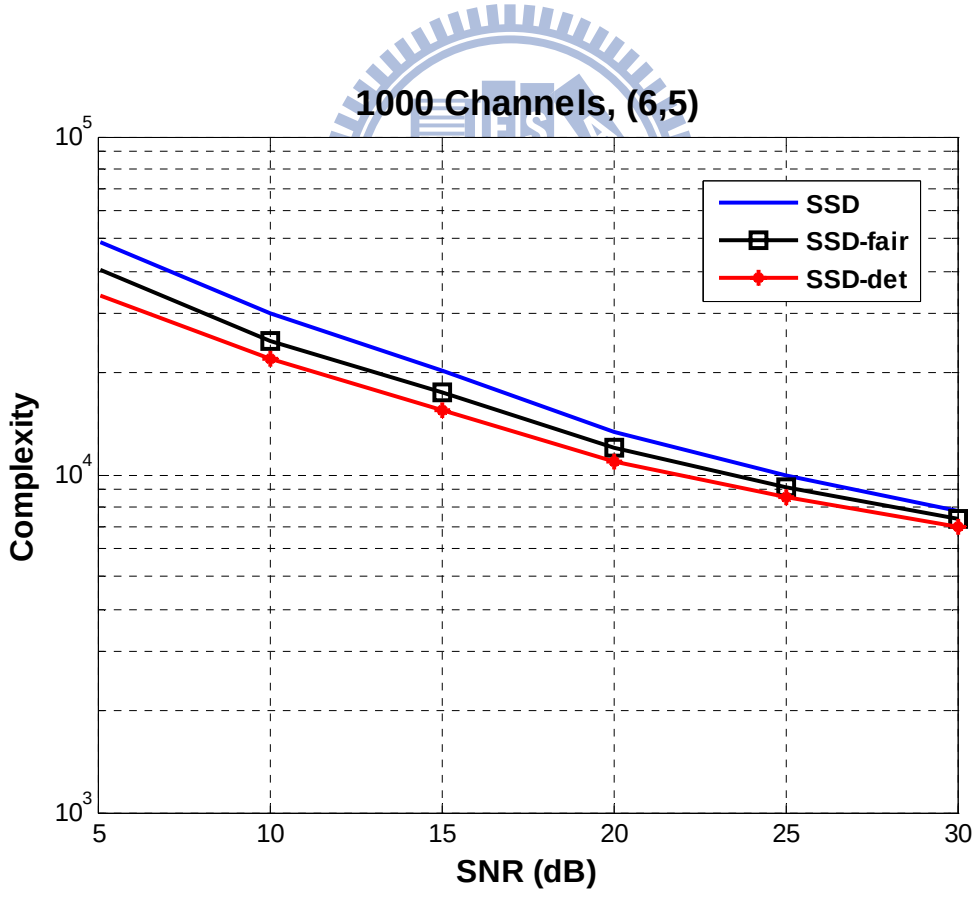

Fig. 4-9 Decoding complexity comparison using SSD at receiver. Transmitter has six antennas, and receiver has five antennas.

Fig. 4-9 shows another simulation of decoding complexity. The transmitter has six antennas, and receiver has five antennas. The other simulation parameters are the same as Fig. 4-8. Because the transmitter and receiver have more antennas, the sizes of the channel matrix become larger. Thus the decoding complexity will increase. The applied SDA in SSD will become a more important role. We can observe that the decoding complexity of SSD can also be reduced by applying the determinant based power allocation at low SNR.

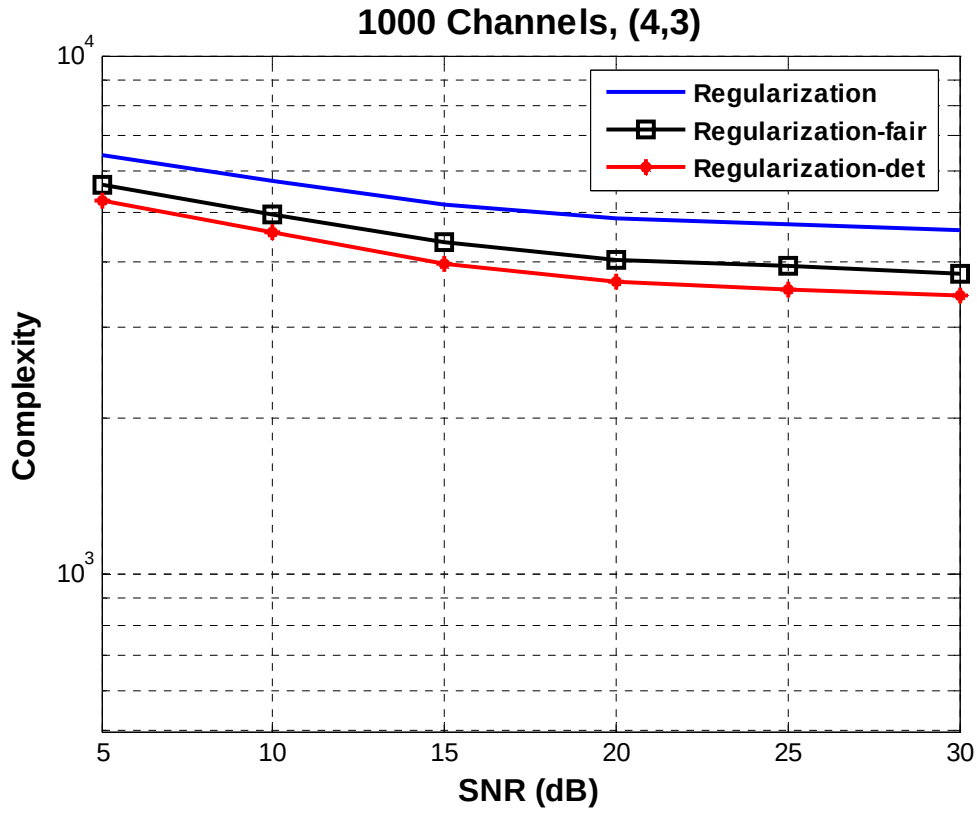

Fig. 4-10 Decoding complexity comparison using regularization method at receiver. Transmitter has four antennas, and receiver has three antennas.

Fig. 4-10 shows the simulation of decoding complexity of the regularization method. We use 16-QAM modulation in 1000 channel realizations. The transmitter has four antennas, and receiver has three antennas. The regularization method transforms the underdetermined problem into an overdetermined problem. Thus the

existing SDA could to applied on the decoding process. Fig. 4-10 shows that the decoding complexity can be reduced with the proposed power allocations applied. Fig. 4-11 shows that the decoding complexity of the regularization method with six transmit antennas and five receive antennas. The other parameters are the same as Fig. 4-10. The numerical result shows that the decoding complexity can also be reduced for a large antenna size with the proposed power allocation applied.

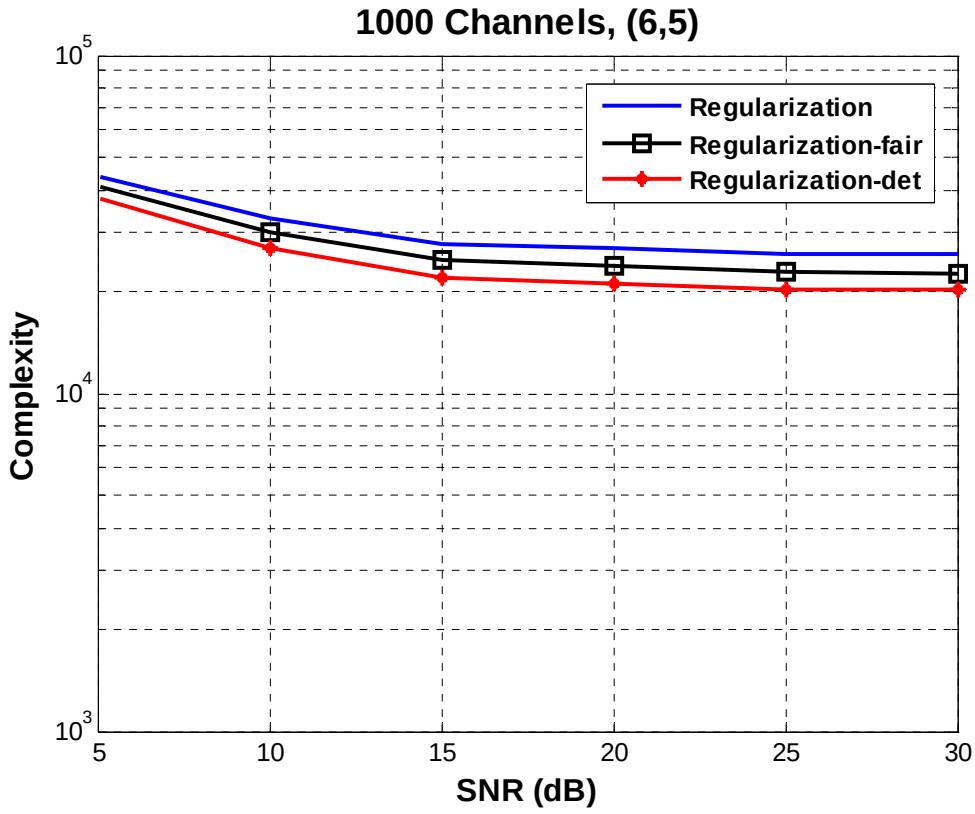

Fig. 4-11 Decoding complexity comparison using regularization method at receiver. Transmitter has six antennas, and receiver has five antennas.

Fig. 4-12 compares the sum rate of four users with different schemes. In the waterfilling power allocation scheme, the utility function is chosen to maximize the sum rate of all users. Thus, the sum rate of the waterfilling scheme is always higher than the other schemes. Although the sum rate of the proposed fairness scheme is

lower than the scheme without power allocation, it could obtain fair rates for all users. With the determinant based power allocation, the condition number of the equivalent channel matrix can be reduced, but the sum rate will be smaller than the sum rate without power allocation.

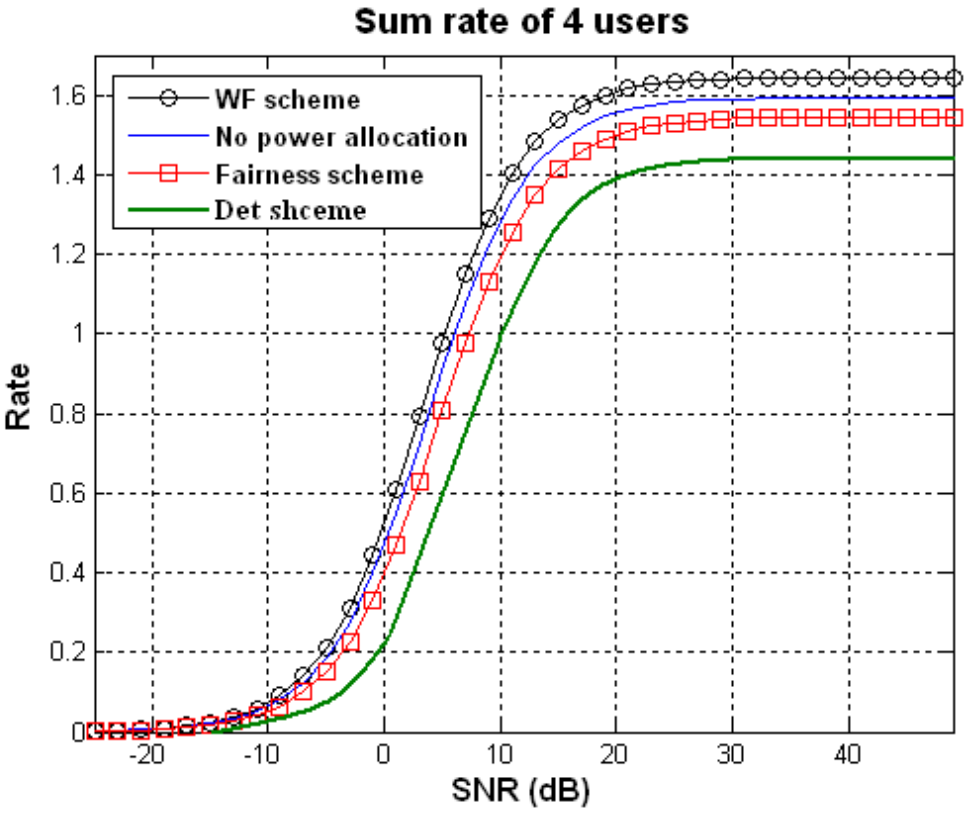

Fig. 4-12 Sum rate comparison for determinant based schemes

4.4 Summary

The condition number of the channel matrix is a critical factor for decoder design in underdetermined MIMO systems. Most efficient decoding algorithms of

underdetermined MIMO systems work with SDA, and thus are sensitive to the condition number. Simulation results show that the fairness power allocation can reduce the condition number of the equivalent channel matrix. Motivated by the fairness scheme, we propose a determinant based utility function to make the eigenvalues close to each other. Thus it can reduce the condition number effectively. Simulations show that the decoding complexity of underdetermined MIMO systems can be reduced with a smaller condition number. Although the decoding complexity can be reduced in underdetermined MIMO systems, the sum rate will be smaller as a price.

Chapter 5

Conclusions and Future Works

In the beginning, this thesis reviews the development of MIMO systems, and the channel capacity of the MIMO systems is introduced. Spatial diversity and spatial multiplexing are two main techniques used in MIMO systems, and can improve the system performance. Several decoding algorithms are proposed for underdetermined MIMO systems. These decoders are developed based on the SDA. Considering uplink MU-MIMO systems, the channel gains will be small when the users are far away from the base station or blocked by obstacles in practical environments. This results in poor data rates for those users. Our goal is to achieve the fair rates for all users.

Since linear precoding techniques cannot be used in the uplink MU-MIMO, we propose a transmit power allocation scheme to achieve the goal. In Chapter 3, we give a detailed description of the proposed transmit power allocation in the MU-MIMO systems. The nonlinear optimization problem is reformulated into a modified form. Thus we can apply the Interior-point algorithm to solve it. The proposed power allocation can also be applied in the SU-MIMO systems. Simulation results show that the fairness based power allocation could provide a higher data rate to the worst condition user than the waterfilling power allocation. This demonstrates a trade-off between the maximum sum rate and user fairness.

The discussion of condition number and the determinant based utility function are given in Chapter 4. If we use the SDA at the receiver, the decoding complexity can be reduced with a smaller condition number. The numerical results show that the fairness scheme tends to obtain a smaller condition number of the equivalent channel matrix. Thus the decoding complexity of the underdetermined MIMO systems could be reduced with the proposed power allocation applied. Motivated by the fairness scheme, we propose a determinant based utility function to reduce the condition number, further reducing the decoding complexity.

The main contributions of this thesis are as follows. We propose a transmit power allocation scheme which provides fair data rates. It improves the poor data rates for users in unfavorable situations. By reformulating the nonlinear optimization problem into a modified form, we can apply the typical Interior-point algorithm to solve it. We observe that the fairness scheme could lead to a small condition number of the equivalent channel matrix, and propose a determinant based utility function trying to equalize the eigenvalues. The decoding complexity of the SDA based decoder for underdetermined MIMO systems can thus be reduced with the proposed power allocation applied.

There are still some issues remaining to be discussed in this work. First, how to find the mathematical relation between the fairness scheme and condition numbers is a concern. Also, how to tackle with imperfect CSI at the receiver is an interesting topic. Furthermore, finding a precoding matrix to minimize the channel condition number is an important subject worthy of investigation.

Bibliography

[1] E. Telatar, "Capacity of multi-antenna Gaussian channels," *AT&T Bell Labs Internal Tech. Memo.*, June 1995.

[2] J. Foschini and M. J. Gans, “On limits of wireless communications in a fading environment when using multiple antennas,” *Wireless Personal Commun.*, vol. 6, no.3, pp. 311-335, Mar. 1998.

[3] S. M. Alamouti, “A simple transmit diversity technique for wireless communications,” *IEEE J. Select. Areas Commun.*, vol. 16, no. 8, pp. 1451-1458, Oct. 1998.

[4] G. J. Foschini, “Layered space-time architecture for wireless communication in a fading environment when using multi-element antennas,” *AT&T Bell Labs Tech. J.*, pp. 41-59, Autumn 1996.

[5] A. J. Goldsmith and S. G. Chua, “Variable-rate variable-power MQAM for fading channels,” *IEEE Trans. Commun.*, vol. 45, no.10, pp. 1218-1230, Oct. 1997.

[6] S. Catreux, V. Erceg, D. Gesbert and R. W. Heath, “Adaptive modulation and MIMO coding for broadband wireless data networks,” *IEEE Commun. Mag.*, vol. 40, no. 6, pp. 108-115, Jun. 2002.

[7] G. J. Foschini, G. D. Golden, R. A. Valenzuela and P. W. Wolniansky, "Simplified processing for high spectral efficiency wireless communication employing multi-element arrays," *IEEE J. Select. Areas Commun.*, vol. 17, no. 11, pp. 1841-1852, Nov. 1999.

[8] G. D. Golden, G. J. Foschini, R. A. Valenzuela and P. W. Wolniansky, "Detection algorithm and initial laboratory results using V-BLAST space-time communication architecture," *Electronic Letters*, vol. 35, no. 1, pp. 14-16, Jan. 1999.

[9] U. Fincke, and M. Pohst, "Improved methods for calculating vectors of short

length in a lattice, including a complexity analysis," *Math. Comput.*, vol. 44, no. 170, pp. 463-471, Apr. 1985.

[10] B. Hassibi and "On the sphere-decoding algorithm I. expected complexity," *IEEE Trans. Signal Process.*, vol. 53, no. 8, pp. 2806-2818, Aug. 2005.

[11] H. Vikalo, and B. Hassibi, " On the sphere-decoding algorithm II. generalizations, second-order statistics, and applications to communications," *IEEE Trans. Signal Process.*, vol. 53, no. 8, pp. 2819-2834, Aug. 2005.

[12] C. P. Schnorr and M. Euchner, "Lattice basis reduction: improved practical algorithms and solving subset sum problems," *Math. Programming*, vol. 66, pp. 181-191, Aug. 1994.

[13] M. O. Damen, K. Abed-Meraim, and J.-C. Belfiore, “A generalised sphere decoder for asymmetrical space–time communication architecture,” *IEE Electronics Letters*, vol. 36, no. 2, pp. 166–167, Jan. 2000.

[14] K. K. Wong and A. Paulraj, “Near maximum-likelihood detection with reduced-complexity for multiple-input single-output antenna systems,” in *Proc. Asilomar Conf. on Signals, Systems, and Computers*, Nov. 2004.

[15] K. K. Wong and A. Paulraj, “Efficient near maximum-likelihood detection for underdetermined MIMO antenna systems using a geometrical approach,” *EURASIP Journal on Wireless Commun. and Networking*, Oct. 2007.

[16] K. K. Wong, A. Paulraj and R. D. Murch, “Efficient high-performance decoding for overloaded MIMO antenna systems,” *IEEE Trans. Wireless Commun.*, vol. 6, no. 5, pp. 1833-1843, May 2007.

[17] T. Cui and C. Tellambura, "An efficient generalized sphere decoder for rank-deficient MIMO systems," *IEEE Commun. Lett.*, vol. 9, no. 5, pp. 423-425, May 2005.

[18] D. P. Palomar, and J. Fonollosa, "Practical algorithms for a family of waterfilling solutions," *IEEE Trans. Signal Process.*, vol. 53, no. 2, pp. 686-695, Feb. 2005.

[19] T. M. Cover and J. A. Thomas, *Elements of Information Theory*, John Wiley & Son, Inc., 1991.

[20] P. W. Wolniansky, G. J. Foschini, G. D. Golden and R. A. Valenzuela, “V-BLAST: An architecture for realizing very high data rates over the rich-scattering wireless channel,” in *Proc. URSI ISSSE-98*,pp. 295-300, 1998.

[20] E. Viterbo, and J. Boutros, “A universal lattice code decoder for fading channels,” *IEEE Trans. Inf. Theory*, vol. 45, no. 5, pp. 1639-1642, July 1999.

[21] F. P. Kelly, A. K. Maulloo and D. K. H. Tan., "Rate control in communication networks: shadow prices, proportional fairness and stability," *Journal of the Operational Research Society,* vol. 49, no. 3, pp. 237-252, Mar. 1998.

[22] H. Zhao, H. Long, and W. Wang, "Combined-weight sphere decoder in bad channel," *Wireless Pervasive Computing, 2006 1st International Symposium on*, pp. 1-3, Jan. 2006.

[23] R. J. Vanderbei and D. F. Shanno, "An interior-point algorithm for nonconvex nonlinear programming," *Research Report SOR-97-21*, Statistics and Operations Res., Princeton University, June 1998.

[24] D. F. Shanno, and R. J. Vanderbei, "Interior-point methods for nonconvex nonlinear programming: orderings and high-order methods," *Research Report SOR-99-5*, Statistics and Operations Res., Princeton University, May 1999.

[25] S. Parker, M. Sandell, M. S. Yee, Y. Sun, M. Ismail, P. Strauch, and J. McGeehan, "Space-time codes for future WLANs: principles, practice, and performance," *IEEE Communications Magazine*,vol. 42, no. 12, pp. 96-103, Dec. 2004.

[26] J. Lim, H. G. Myung, K. Oh, and D. J. Goodman, "Proportional fair scheduling of uplink single-carrier FDMA systems," *Personal, Indoor and Mobile Radio Commun., IEEE 17th International Symposium on*,pp. 1-6, Sept. 2006.